

# Hierarchical Neural Networks, $p$ -Adic PDEs, and Applications to Image Processing

W. A. Zúñiga-Galindo\*

University of Texas Rio Grande Valley  
School of Mathematical and Statistical Sciences  
One West University Blvd.,  
Brownsville, TX 78520, United States.  
wilson.zunigagalindo@utrgv.edu

B. A. Zambrano-Luna

University of Alberta  
Department of Mathematical and Statistical Sciences  
CAB 632  
Edmonton, Alberta, Canada T6G 2G1  
bzambran@ualberta.ca

Baboucarr Dibba

University of Texas Rio Grande Valley  
School of Mathematical and Statistical Sciences  
One West University Blvd.,  
Brownsville, TX 78520, United States.  
baboucarr.dibba01@utrgv.edu

June 13, 2024

## Abstract

The first goal of this article is to introduce a new type of  $p$ -adic reaction-diffusion cellular neural network with delay. We study the stability of these networks and provide numerical simulations of their responses. The second goal is to provide a quick review of the state of the art of  $p$ -adic cellular neural networks and their applications to image processing.

---

\*The first and third authors were partially supported by the Lokenath Debnath Endowed Professorship.

# 1 Introduction

This article has twofold purposes. First, it continues the investigation of the first two authors on  $p$ -adic cellular neural networks (CNNs) and their application to image processing; see [1]-[2]. The  $p$ -adic CNNs are hierarchical generalizations of the classical CNNs introduced by Chuan and Yang in the 1980s; see [3]-[6], and the references therein. The classical CNNs are given by a set of integrodifferential equations controlling the states of the neurons forming the network. Typically, the neurons are organized in a lattice contained in  $\mathbb{R}^2$ . The  $p$ -adic integers,  $\mathbb{Z}_p$ , forms an infinite rooted tree. The neurons are naturally organized in layers (levels), and by cutting the tree  $\mathbb{Z}_p$  at level  $l \geq 1$ , one obtains a finite rooted tree  $G_l$  with  $l$  levels and  $p^l$  vertices at the top level. In the  $p$ -adic CNNs the neurons are organized in a finite rooted tree,  $G_l$ . In the limit when the number of neurons tends to infinity, the  $p$ -adic CNNs admit limits that are abstract evolution integrodifferential equations on  $\mathbb{Z}_p$ . This type of equation can be studied using standard techniques for PDEs. In this article, we studied  $p$ -adic reaction-diffusion CNNs with delay, see Section 4. We study the Cauchy problem and the stability of the new networks. We also provide numerical simulations for the solutions of these networks. Our numerical results show a chaotic behavior in the responses of the  $p$ -adic CNNs with delay.

The second goal is to quickly review the state of the art in  $p$ -adic CNNs and their applications to image processing. The  $p$ -adic CNNs are bioinspired by the Wilson-Cowan models for the macroscopic activity patterns in the cortex of mammals and invertebrates; see, e.g., [7], and the references therein. The formulation of the discrete Wilson-Cowan models does not require a particular topology for the neurons. For instance, these models are valid for neural networks (NNs) with hierarchical topologies. However, when taking the limit when the numbers of neurons tend to infinity, in most of the available literature, it is assumed that neurons are organized in lattice contained in  $\mathbb{R}^n$ ; this is done to approximate certain sums by Riemann–Stieltjes integrals.

Based on experimental data, it has been hypothesized that cortical neural networks are arranged in fractal or self-similar patterns and have the small-world property, see, e.g., [8]-[18], and the references therein. These properties are incompatible with the standard Wilson-Cowan models formulated on  $(\mathbb{R}^n, +)$ . To overcome this problem, it is necessary to assume that the neurons are organized hierarchically, which requires to change the additive group  $(\mathbb{R}^n, +)$  for an hierarchical additive group. In [19], the first two authors formulated a  $p$ -adic version of the Wilson-Cowan models on the group  $(\mathbb{Z}_p, +)$ , and showed that this model is a good substitute of the standard one, where the cortical neural networks are arranged in self-similar patterns and have the small-world property. The  $p$ -adic CNNs are simplified versions of the  $p$ -adic Wilson-Cowan models that have showed a great potential to perform several tasks in image processing. Finally, we present some relevant research problems connecting  $p$ -adic NNs with image processing and neuronal dynamics.

## 2 Motivations and Preliminaries

In this section, we discuss the motivations behind the study of hierarchical biological and artificial NNs using methods of non-Archimedean analysis.

### 2.1 PDE based models for neural fields

The spatiotemporal continuum models for the dynamics of macroscopic activity patterns in the cortex were introduced in the 1970s following the seminal work by Wilson and Cowan, Amari, among others, see, e.g., [20]-[22], see also [7] and the references therein. Such models take the form of integrodifferential evolution equations in which the integration kernels represent the strength of the connection between neurons, or more generally, the spatial distribution of synaptic connections between different neural populations, and the state macroscopic variables represent some average of neural activity. These PDEs based models have been used to model phenomena such as short-term memory [23], the head direction system [24], visual hallucinations [25]-[26], and EEG rhythms [27].

The simplest continuous model in one spatial dimension is

$$\frac{\partial u(x, t)}{\partial t} = -u(x, t) + \int_{-\infty}^{\infty} w(x - y) f(u(y, t)) dy, \quad (1)$$

where at the position  $x \in \mathbb{R}$  there is a group of neurons, and  $u(x, t)$  is some average network activity at the time  $t \in \mathbb{R}_+ := \{s \in \mathbb{R}; s \geq 0\}$ . The kernel  $w$  gives the strength of connection between the neurons located at the position  $x$  and  $y$ . In the simplest model  $w$  is symmetric, i.e.  $w(x) = w(-x)$ ,  $\lim_{x \rightarrow \infty} w(x) = 0$ ,  $\int_{-\infty}^{\infty} w(x) dx < \infty$ , and continuous. The non-linear function  $f$  is the activation (or firing) function. For instance, a non-decreasing function satisfying  $\lim_{s \rightarrow -\infty} f(s) = 0$ ,  $\lim_{s \rightarrow \infty} f(s) = 1$ . The amount  $f(u(x, t))$  is the firing rate normalized to one. The integral of  $w(x - y) f(u(y, t))$  over  $y$  represents the influence of all neurons at position  $y$  on the neurons at position  $x$ .

There are two basic discrete models. The first one is the voltage-based rate model:

$$\tau_m \frac{\partial a_i(t)}{\partial t} = -a_i(t) + \sum_j w_{ij} f(a_j(t)), \quad (2)$$

where  $\tau_m$  is a time constant and  $w_{ij}$  is the strength between neurons  $i$  and  $j$ . The second one is called the activity-based model, it has the form

$$\tau_s \frac{\partial v_i(t)}{\partial t} = -v_i(t) + f\left(\sum_j w_{ij} v_j(t)\right), \quad (3)$$

where  $\tau_s$  is a time constant. The reader may consult [28] for an in-depth discussion about these two models. *A fundamental observation is that in these models, the topology of the neurons (the architecture of the network) is arbitrary.* For instance, the neurons may be organized in a hierarchical tree-like

structure. The continuous versions of the models (2)-(3) are obtained by taking the limit when the number of neurons tends to infinity. In the limit, the discrete variable  $i$  becomes a continuous variable  $x$ . Almost all the published literature assumes that the neurons are organized in a lattice contained in  $\mathbb{R}^n$ . Using this hypothesis, the sums in (2)-(3) become Riemann–Stieltjes integrals in the limit when the number of neurons tends to infinity:

$$\begin{aligned}\tau_m \frac{\partial a(x, t)}{\partial t} &= -a(x, t) + \int_{-\infty}^{\infty} w(x, y) f(a(y, t)) dy, \\ \tau_s \frac{\partial v(x, t)}{\partial t} &= -v(x, t) + f\left(\int_{-\infty}^{\infty} w(x, y) v(y, t) dy\right),\end{aligned}$$

where  $x \in \mathbb{R}$ ,  $t \in \mathbb{R}_+$ . In particular, this approach discards any hierarchical organization of the neurons.

The Wilson-Cowan model describes the evolution of excitatory and inhibitory activity in a synaptically coupled neuronal network. The model is given by the following system of non-linear integro-differential evolution equations:

$$\left\{ \begin{array}{l} \tau \frac{\partial E(x, t)}{\partial t} = -E(x, t) + \\ (1 - r_E E(x, t)) f_E(w_{EE}(x) * E(x, t) - w_{EI}(x) * I(x, t) + h_E(x, t)) \\ \tau \frac{\partial I(x, t)}{\partial t} = -I(x, t) + \\ (1 - r_I I(x, t)) f_I(w_{IE}(x) * E(x, t) - w_{II}(x) * I(x, t) + h_I(x, t)), \end{array} \right. \quad (4)$$

where  $E(x, t)$  is a temporal coarse-grained variable describing the proportion of excitatory neuron firing per unit of time at position  $x \in \mathbb{R}$  at the instant  $t \in \mathbb{R}_+$ . Similarly the variable  $I(x, t)$  represents the activity of the inhibitory population of neurons. The ‘\*’ denotes the spatial convolution. The main parameters of the model are the strength of the connections between each subtype of population ( $w_{EE}$ ,  $w_{IE}$ ,  $w_{EI}$ ,  $w_{II}$ ) and the strength of input to each subpopulation ( $h_E(x, t)$ ,  $h_I(x, t)$ ). This model generates a diversity of dynamical behaviors that are representative of observed activity in the brain, like multistability, oscillations, traveling waves, and spatial patterns, see, e.g., [7] and the references therein.

## 2.2 Neurons geometry and small-world networks

Nowadays, there are extensive databases of neuronal wiring diagrams (connection matrices) of the invertebrates’ and mammals’ cerebral cortexes. The connection matrices are adjacency matrices of weighted directed graphs, where the vertices represent neuron populations or regions in a cortex. These matrices correspond to the kernels  $w_{AB}$ ,  $A, B \in \{E, I\}$ , in model (4), or to the kernels  $w_{ij}$  in models (2)-(3). Based on these data, several researchers hypothesized

that cortical neural networks are arranged in fractal or self-similar patterns and have the small-world property, see, e.g., [8]-[18], and the references therein. It is widely accepted that the brain is a small-world network, see, e.g., [9]-[12], and the references therein. The small-worldness is believed to be a crucial aspect of efficient brain organization that confers significant advantages in signal processing, furthermore, the small-world organization is deemed essential for healthy brain function, see, e.g., [11], and the references therein. A small-world network has a topology that produces short paths across the whole network, i.e., given two nodes, there is a short path between them (the six degrees of separation phenomenon). In turn, this implies the existence of long-range interactions in the network.

The compatibility of the Wilson-Cowan type models with the small-world network property requires a non-negligible interaction between any two groups of neurons, i.e.,  $w_{AB}(x) > \varepsilon > 0$ , for any  $x$ , and for  $A, B \in \{E, I\}$ , where the constant  $\varepsilon > 0$  is independent of  $x$ . Since the kernels  $w_{AB}$  should be integrable, such as we pointed out in the simplest model (3), then, it is necessary to replace  $(\mathbb{R}, +)$  by a compact subgroup, however,  $(\mathbb{R}, +)$  does not have non-trivial subgroups, and consequently, the Wilson-Cowan models on  $(\mathbb{R}, +)$  are not compatible with small-world network property.

### 2.3 Cellular neural Networks and complex multi-level systems

In the late 80s Chua and Yang introduced a new natural computing paradigm called the cellular neural networks CNN which includes the cellular automata as a particular case. This paradigm has been extremely successful in various applications in vision, robotics and remote sensing, etc. See [3]-[6] and the references therein.

Let  $(\mathcal{M}, |\cdot|)$  be a normed  $\mathbb{R}$ -vector space, where  $\mathcal{M}$  is a finite set. An element  $i$  of  $\mathcal{M}$  is called a cell. A discrete CNN is a dynamical system  $\text{CNN}(\mathbb{A}, \mathbb{B}, U, Z)$  on  $\mathcal{M}$ . The state  $X(i, t) \in \mathbb{R}$  of cell  $i$  is described by the following system of differential equations:

(i) state equation:

$$\frac{dX(i, t)}{dt} = -X(i, t) + \sum_{j \in \mathcal{M}} \mathbb{A}(i, j)Y(j, t) + \sum_{j \in \mathcal{M}} \mathbb{B}(i, j)U(j) + Z(i), \quad i \in \mathcal{M},$$

(ii) output equation:

$$Y(i, t) = f(X(i, t)), \quad i \in \mathcal{M},$$

where  $Y(i, t) \in \mathbb{R}$  is the output of cell  $i$  at the time  $t$ ,  $f : \mathbb{R} \rightarrow \mathbb{R}$  is a bounded Lipschitz function satisfying  $f(0) = 0$ . The function  $U(i) \in \mathbb{R}$  is the input of the cell  $i$ ,  $Z(i) \in \mathbb{R}$  is the threshold of cell  $i$ , and  $\mathbb{A}, \mathbb{B} : \mathcal{M} \times \mathcal{M} \rightarrow \mathbb{R}$  are the feedback operator and feedforward operator, respectively.

Not all the cells of  $\mathcal{M}$  are active. A cell  $i$  is connected with cell  $j$  if  $\mathbb{A}(i, j) \neq 0$  or  $\mathbb{B}(i, j) \neq 0$  for some  $j \in \mathcal{M}$ . Then, a  $p$ -adic discrete CNN is a dynamical system on

$$C_{\mathcal{M}} := \{i \in \mathcal{M}; \mathbb{A}(i, j) \neq 0 \text{ or } \mathbb{B}(i, j) \neq 0 \text{ for some } j \in \mathcal{M}\}.$$

The topology of a  $p$ -adic discrete CNN depends on the functions  $\mathbb{A}, \mathbb{B} : \mathcal{M} \times \mathcal{M} \rightarrow \mathbb{R}$ . The discrete CNNs satisfying

$$\mathbb{A}(i, j) = \mathbb{A}(|i - j|), \mathbb{B}(i, j) = \mathbb{B}(|i - j|), \quad (5)$$

which are discrete CNNs having the space-invariant property.

The CNNs are bioinspired on the Wilson-Cowan models; see (2). Most of the literature about CNNs is dedicated to the study and applications of NNs whose topology comes from a finite lattice contained in some  $\mathbb{R}^n$ . We already pointed out that it is widely accepted that hierarchical organization plays a central role in biological NNs. Since most artificial NNs are bioinspired, it is natural to conclude that hierarchical artificial NNs are relevant computational paradigms. We propose to study hierarchical NNs as complex multi-level systems. These systems are made up of several subsystems and are characterized by emergent behavior resulting from nonlinear interactions between subsystems for multiple levels of organization; see, e.g., [29]-[30], and the references therein.

An non-Archimedean vector space  $(M, \|\cdot\|)$  is a normed vector space whose norm satisfies

$$\|x + y\| \leq \max\{\|x\|, \|y\|\},$$

for any two vectors  $x, y$  in  $M$ . In such a space, the balls are organized in a hierarchical form. This type of space plays a central role in formulating models of complex multi-level systems. The field of  $p$ -adic numbers  $\mathbb{Q}_p$  and the field of formal Laurent series  $\mathbb{F}_p((T))$  are paramount examples of non-Archimedean vector spaces. Methods of non-Archimedean analysis have been successfully used to construct models for hierarchical NNs; see, e.g., [31]-[38], and the references therein.

## 2.4 $p$ -Adic numbers and tree-like structures

This section reviews some basic results on  $p$ -adic analysis required in this article. For a detailed exposition on  $p$ -adic analysis, the reader may consult [39]-[41].

### 2.4.1 $p$ -Adic integers

From now on,  $p$  denotes a fixed prime number. The ring of  $p$ -adic integers  $\mathbb{Z}_p$  is defined as the completion of the ring of integers  $\mathbb{Z}$  with respect to the  $p$ -adic norm  $|\cdot|_p$ , which is defined as

$$|x|_p = \begin{cases} 0 & \text{if } x = 0 \\ p^{-\gamma} & \text{if } x = p^\gamma a \in \mathbb{Z}, \end{cases} \quad (6)$$

where  $a$  is an integer coprime with  $p$ . The integer  $\gamma = \text{ord}_p(x) := \text{ord}(x)$ , with  $\text{ord}(0) := +\infty$ , is called the  $p$ -adic order of  $x$ .

Any non-zero  $p$ -adic integer  $x$  has a unique expansion of the form

$$x = x_k p^k + x_{k+1} p^{k+1} + \dots,$$

with  $x_k \neq 0$ , where  $k$  is a non-negative integer, and the  $x_j$ s are numbers from the set  $\{0, 1, \dots, p-1\}$ . There are natural field operations, sum, and multiplication, on  $p$ -adic integers. The norm  $|\cdot|_p$ , see (6), extends to  $\mathbb{Z}_p$  as  $|x|_p = p^{-k}$  for a nonzero  $p$ -adic integer  $x$ .

The metric space  $(\mathbb{Z}_p, |\cdot|_p)$  is a complete ultrametric space. Ultrametric means that  $|x+y|_p \leq \max\{|x|_p, |y|_p\}$ . As a topological space  $\mathbb{Z}_p$  is homeomorphic to a Cantor-like subset of the real line, see Figure 1, and the references [39]-[40], [42].

For  $r \in \mathbb{N}$ , denote by  $B_{-r}(a) = \{x \in \mathbb{Z}_p; |x-a|_p \leq p^{-r}\}$  the ball of radius  $p^{-r}$  with center at  $a \in \mathbb{Z}_p$ , and take  $B_{-r}(0) := B_{-r}$ . The ball  $B_0$  equals the ring of  $p$ -adic integers  $\mathbb{Z}_p$  (the unit ball). We use  $\Omega(p^r |x-a|_p)$  to denote the characteristic function of the ball  $B_{-r}(a)$ . Two balls in  $\mathbb{Z}_p$  are either disjoint or one is contained in the other. The balls are compact subsets, thus  $(\mathbb{Z}_p, |\cdot|_p)$  is a compact topological space.

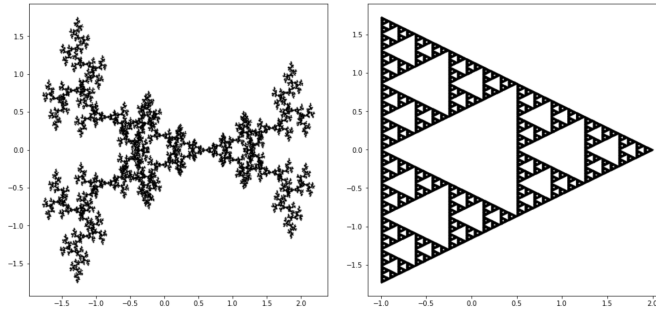


Figure 1: Based upon [42], we construct an embedding  $f: \mathbb{Z}_p \rightarrow \mathbb{R}^2$ . The figure shows the images of  $f(\mathbb{Z}_2)$  and  $f(\mathbb{Z}_3)$ . This computation requires a truncation of the  $p$ -adic integers. We use  $\mathbb{Z}_2/2^{14}\mathbb{Z}_2$  and  $\mathbb{Z}_3/3^{10}\mathbb{Z}_3$ , respectively.

#### 2.4.2 Tree-like structures

The set of  $p$ -adic integers modulo  $p^l$ ,  $l \geq 1$ , consists of all the integers of the form  $i = i_0 + i_1 p + \dots + i_{l-1} p^{l-1}$ . These numbers form a complete set of representatives for the elements of the additive group  $G_l = \mathbb{Z}_p/p^l \mathbb{Z}_p$ , which is isomorphic to the set of integers  $\mathbb{Z}/p^l \mathbb{Z}$  (written in base  $p$ ) modulo  $p^l$ . By restricting  $|\cdot|_p$  to  $G_l$ , it

becomes a normed space, and  $|G_l|_p = \{0, p^{-(l-1)}, \dots, p^{-1}, 1\}$ . With the metric induced by  $|\cdot|_p$ ,  $G_l$  becomes a finite ultrametric space. In addition,  $G_l$  can be identified with the set of branches (vertices at the top level) of a rooted tree with  $l$  levels and  $p^l$  branches. By definition, the tree's root is the only vertex at level 0. There are exactly  $p$  vertices at level 1, which correspond with the possible values of the digit  $i_0$  in the  $p$ -adic expansion of  $i$ . Each of these vertices is connected to the root by a non-directed edge. At level  $k$ , with  $2 \leq k \leq l-1$ , there are exactly  $p^k$  vertices, each vertex corresponds to a truncated expansion of  $i$  of the form  $i_0 + \dots + i_{k-1}p^{k-1}$ . The vertex corresponding to  $i_0 + \dots + i_{k-1}p^{k-1}$  is connected to a vertex  $i'_0 + \dots + i'_{k-2}p^{k-2}$  at the level  $k-1$  if and only if  $(i_0 + \dots + i_{k-1}p^{k-1}) - (i'_0 + \dots + i'_{k-2}p^{k-2})$  is divisible by  $p^{k-1}$ . See Figure 1. The balls  $B_{-r}(a) = a + p^r\mathbb{Z}_p$  are infinite rooted trees.

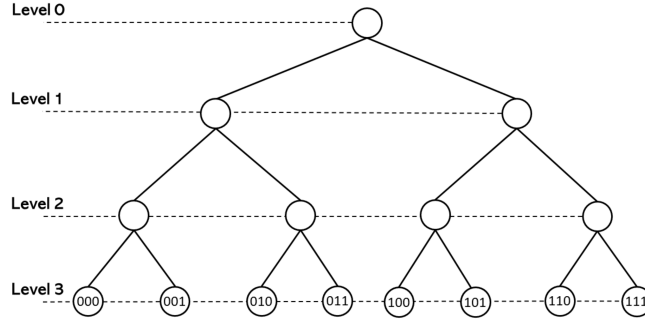


Figure 2: The rooted tree associated with the group  $\mathbb{Z}_2/2^3\mathbb{Z}_2$ . The elements of  $\mathbb{Z}_2/2^3\mathbb{Z}_2$  have the form  $i = i_0 + i_12 + i_22^2$ ,  $i_0, i_1, i_2 \in \{0, 1\}$ . The distance satisfies  $-\log_2 |i - j|_2 = \text{level of the first common ancestor of } i, j$ . Figure taken from [33]

### 2.4.3 The Bruhat-Schwartz space in the unit ball

A real-valued function  $\varphi$  defined on  $\mathbb{Z}_p$  is called *Bruhat-Schwartz function* (or a *test function*) if for any  $x \in \mathbb{Z}_p$  there exist an integer  $l \in \mathbb{N} = \{0, 1, \dots\}$  such that

$$\varphi(x + x') = \varphi(x) \text{ for any } x' \in B_l. \quad (7)$$

The  $\mathbb{R}$ -vector space of Bruhat-Schwartz functions supported in the unit ball is denoted by  $\mathcal{D}(\mathbb{Z}_p)$ . For  $\varphi \in \mathcal{D}(\mathbb{Z}_p)$ , the largest number  $l = l(\varphi)$  satisfying (7) is called *the exponent of local constancy* (or *the parameter of constancy*) of  $\varphi$ . A test function with exponent of local constancy  $l$  has the form

$$\varphi(x) = \sum_{i \in G_l} \varphi(i) \Omega\left(p^l |x - i|_p\right), \quad \varphi(i) \in \mathbb{R},$$



where  $i = i_0 + i_1p + \dots + i_{l-1}p^{l-1} \in G_l = \mathbb{Z}_p/p^l\mathbb{Z}_p$ . Notice that if  $l = 0$ ,  $G_0 = \{0\}$ . These functions form a finite dimensional vector space  $\mathcal{D}^l(\mathbb{Z}_p)$  spanned by the basis  $\left\{ \Omega \left( p^l |x - i|_p \right) \right\}_{i \in G_l}$ . By identifying  $\varphi \in \mathcal{D}^l(\mathbb{Z}_p)$  with the column vector  $[\varphi(i)]_{i \in G_l} \in \mathbb{R}^{\#G_l}$ , we get that  $\mathcal{D}^l(\mathbb{Z}_p)$  is isomorphic (as Banach space) to  $\mathbb{R}^{\#G_l}$  endowed with the norm

$$\left\| [\varphi(i)]_{i \in G_l} \right\| = \max_{i \in G_l} |\varphi(i)|.$$

Furthermore,

$$\mathcal{D}^l \hookrightarrow \mathcal{D}^{l+1} \hookrightarrow \mathcal{D}(\mathbb{Z}_p),$$

where  $\hookrightarrow$  denotes a continuous embedding, and  $\mathcal{D}(\mathbb{Z}_p) = \cup_{l \in \mathbb{N}} \mathcal{D}^l(\mathbb{Z}_p)$ .

#### 2.4.4 The Haar measure

Since  $(\mathbb{Z}_p, +)$  is a compact topological group, there exists a Haar measure  $dx$ , which is invariant under translations, i.e.,  $d(x+a) = dx$ , [43]. If we normalize this measure by the condition  $\int_{\mathbb{Z}_p} dx = 1$ , then  $dx$  is unique. It follows immediately that

$$\int_{B_{-r}(a)} dx = \int_{a+p^r\mathbb{Z}_p} dx = p^{-r} \int_{\mathbb{Z}_p} dy = p^{-r}, \quad r \in \mathbb{N}.$$

In a few occasions, we use the two-dimensional Haar measure  $dx dy$  of the additive group  $(\mathbb{Z}_p \times \mathbb{Z}_p, +)$  normalize this measure by the condition  $\int_{\mathbb{Z}_p} \int_{\mathbb{Z}_p} dx dy = 1$ .

#### 2.4.5 Other function spaces

The space  $\mathcal{D}(\mathbb{Z}_p)$  is dense in

$$L^\rho(\mathbb{Z}_p) = L^\rho = \left\{ \varphi : \mathbb{Z}_p \rightarrow \mathbb{R}; \left( \int_{\mathbb{Z}_p} |\varphi(x)|^\rho dx \right)^{\frac{1}{\rho}} < \infty \right\},$$

for  $1 \leq \rho < \infty$ , see e.g. [39, Section 4.3].

We denote by  $C(\mathbb{Z}_p)$  the  $\mathbb{R}$ -vector space of continuous functions defined on  $\mathbb{Z}_p$ . The space of test functions  $\mathcal{D}(\mathbb{Z}_p)$  is dense in  $C(\mathbb{Z}_p)$  with respect to the norm  $\|\phi\|_\infty = \sup_{x \in \mathbb{Z}_p} |\phi(x)|$ . When formulating solutions of initial value problems, the notation  $C(\mathbb{Z}_p, \mathbb{R})$  will be also used.

### 3 $p$ -Adic continuous CNNs

In this section, we quickly review some of the results of [1]. Initially, these results were formulated in  $\mathbb{Q}_p^N$ , but here we reformulate them in  $\mathbb{Z}_p$ . The adaption is straightforward.

We say that a function  $f : \mathbb{R} \rightarrow \mathbb{R}$  is called a Lipschitz function if there exists a real constant  $L(f) > 0$  such that, for all  $x, y \in \mathbb{R}$ ,  $|f(x) - f(y)| \leq L(f)|x - y|$ . We assume  $f(0) = 0$ . A relevant example is

$$f(x) = \frac{1}{2} (|x + 1| - |x - 1|).$$

We define  $\mathcal{X}_\infty(\mathbb{Z}_p) := \mathcal{X}_\infty = (C(\mathbb{Z}_p), \|\cdot\|_\infty)$ , where  $\|\phi\|_\infty = \sup_{x \in \mathbb{Z}_p} |\phi(x)|$ , and  $\mathcal{X}_M := (\mathcal{D}^M(\mathbb{Z}_p), \|\cdot\|_\infty)$  for  $M \geq 1$ . The spaces  $\mathcal{X}_\infty$  and  $\mathcal{X}_M$  are Banach spaces.

Given  $A(x, y), B(x, y) \in L^1(\mathbb{Z}_p \times \mathbb{Z}_p)$ , and  $U, Z \in \mathcal{X}_\infty$ , a  $p$ -adic continuous CNN, denoted as  $\text{CNN}(A, B, U, Z)$ , is the dynamical system given by the following integrodifferential equations: (i) state equation:

$$\frac{\partial X(x, t)}{\partial t} = -X(x, t) + \int_{\mathbb{Z}_p} A(x, y)Y(y, t)dy + \int_{\mathbb{Z}_p} B(x, y)U(y)dy + Z(x), \quad (8)$$

where  $x \in \mathbb{Z}_p$ ,  $t \geq 0$ , and (ii) output equation:  $Y(x, t) = f(X(x, t))$ . We say that  $X(x, t) \in \mathbb{R}$  is the *state of cell*  $x$  at the time  $t$ ,  $Y(x, t) \in \mathbb{R}$  is the *output of cell*  $x$  at the time  $t$ . Function  $A(x, y)$  is the *kernel of the feedback operator*, while function  $B(x, y)$  is the *kernel of the feedforward operator*. Function  $U$  is the *input of the CNN*, while function  $Z$  is the *threshold of the CNN*.

We focus mainly in continuous CNNs having the space invariant property, i.e.  $A(x, y) = A(|x - y|_p)$  and  $B(x, y) = B(|x - y|_p)$  for some  $A, B \in L^1$ , however our results are valid for general  $p$ -adic continuous CNNs.

### 3.1 Discretization of $p$ -adic continuous CNNs

The  $p$ -adic continuous CNNs are mathematical models of hierarchical CNNs. For practical purposes, discrete versions of them are required. By the Hölder inequality,

$$\mathcal{D}(\mathbb{Z}_p) \subset C(\mathbb{Z}_p) \subset L^\rho(\mathbb{Z}_p) \subset L^1(\mathbb{Z}_p), \text{ for } \rho \in (1, \infty],$$

with  $\mathcal{D}(\mathbb{Z}_p)$  dense in  $L^1(\mathbb{Z}_p)$ . Then, any function  $f \in L^\rho(\mathbb{Z}_p)$ ,  $\rho \in [1, \infty]$ , can be approximated in the norm  $\|\cdot\|_\rho$  by a function from  $\mathcal{D}^l(\mathbb{Z}_p) \subset \mathcal{D}(\mathbb{Z}_p)$ , for some  $l \geq 1$ . For this reason, a discretization of a  $p$ -adic continuous  $\text{CNN}(A, B, U, Z)$  is obtained assuming that  $X(\cdot, t)$ ,  $A$ ,  $Y(\cdot, t)$ ,  $B$ ,  $U$  and  $Z$  belong to  $\mathcal{D}^l(\mathbb{Z}_p)$ , i.e.

$$\begin{aligned} X(x, t) &= \sum_{i \in G_l} X(i, t) \Omega(p^l |x - i|_p), \quad Y(x, t) = \sum_{i \in G_l} Y(i, t) \Omega(p^l |x - i|_p), \\ U(x) &= \sum_{i \in G_l} U(i) \Omega(p^l |x - i|_p), \quad Z(x) = \sum_{i \in G_l} Z(i) \Omega(p^l |x - i|_p), \\ A(x, y) &= \sum_{i \in G_l} \sum_{j \in G_l} A(i, j) \Omega(p^l |x - i|_p) \Omega(p^l |y - j|_p), \\ B(x, y) &= \sum_{i \in G_l} \sum_{j \in G_l} B(i, j) \Omega(p^l |x - i|_p) \Omega(p^l |y - j|_p). \end{aligned}$$

On the other hand, if  $f : \mathbb{R} \rightarrow \mathbb{R}$ , then

$$f(X(x, t)) = \sum_{i \in G_l} f(X(i, t)) \Omega(p^l |x - i|_p) = Y(x, t).$$

Now,

$$\frac{\partial}{\partial t} X(x, t) = \sum_{i \in G_l} \frac{\partial}{\partial t} X(i, t) \Omega(p^l |x - i|_p),$$

and

$$\begin{aligned} & \int_{\mathbb{Z}_p} A(x, y) f(X(y, t)) dy \\ &= \sum_{i \in G_l} \left\{ \sum_{j \in G_l} A(i, j) f(X(j, t)) \int_{\mathbb{Z}_p} \Omega(p^l |y - j|_p) dy \right\} \Omega(p^l |x - i|_p) \\ &= p^{-l} \sum_{i \in G_l} \left\{ \sum_{j \in G_l} A(i, j) Y(j, t) \right\} \Omega(p^l |x - i|_p). \end{aligned}$$

Similarly,

$$\int_{\mathbb{Z}_p} B(x, y) U(y) dy = p^{-l} \sum_{i \in G_l} \left\{ \sum_{j \in G_l} B(i, j) U(j) \right\} \Omega(p^l |x - i|_p).$$

Therefore,

$$\frac{\partial}{\partial t} X(i, t) = -X(i, t) + \sum_{j \in G_l} p^{-l} A(i, j) Y(j, t) + \sum_{j \in G_l} p^{-l} B(i, j) U(j) + Z(i),$$

for  $i \in G_l$ , and  $Y(i, t) = f(X(i, t))$ , for  $i \in G_l$ . This is exactly a  $p$ -adic discrete CNN with  $\mathcal{M} = G_l$ ,  $|x - y| = |x - y|_p$ ,  $\mathbb{A}(i, j) = p^{-l} A(i, j)$ ,  $\mathbb{B}(i, j) = p^{-l} B(i, j)$ . Notice that a  $p$ -adic discrete CNN is a dynamical system on

$$C_l := \{i \in G_l; \mathbb{A}(i, j) \neq 0 \text{ or } \mathbb{B}(i, j) \neq 0 \text{ for some } j \in G_l\};$$

see Figure 3. Intuitively a  $p$ -adic continuous CNN has infinitely many layers, each layer corresponds to some  $l$ , which are organized in a hierarchical structure. For practical purposes, a  $p$ -adic continuous CNN is realized as a  $p$ -adic discrete CNN for  $l$  sufficiently large.

### 3.2 Stability of $p$ -adic continuous CNN

We assume that  $A(|x|_p), B(|x|_p) \in L^1(\mathbb{Z}_p)$  are radial functions and that  $U, Z \in \mathcal{X}_\infty$ .

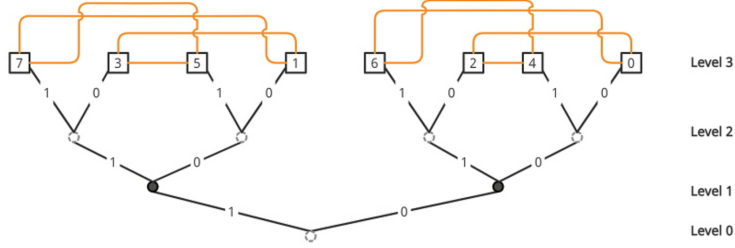


Figure 3: A discrete 2-adic CNN with 8 cells:  $C_3 = \{0, 1, 2, 3, 4, 5, 7\} \subset \mathbb{Z}_2/2^3\mathbb{Z}_2 \subset 2^{-3}\mathbb{Z}_2/2^3\mathbb{Z}_2$ . We set  $\mathbb{B} = 0$  and  $\mathbb{A}(i, j) = [a_{i,j}]$ , with  $a_{i,j} \neq 0$  if  $|i - j|_2 = 1/2$  and  $i, j \in C_3$ ;  $a_{i,j} = 0$  otherwise. Taken from [1]

For  $g \in \mathcal{X}_\infty$ , set

$$\mathbf{H}(g) := \int_{\mathbb{Z}_p} A(|x - y|_p) f(g(y)) dy + \int_{\mathbb{Z}_p} B(|x - y|_p) U(y) dy + Z(x).$$

Then  $\mathbf{H} : \mathcal{X}_\infty \rightarrow \mathcal{X}_\infty$  is a well-defined operator satisfying

$$\|\mathbf{H}(g) - \mathbf{H}(g')\|_\infty \leq L(f) \|A\|_1 \|g - g'\|_\infty, \text{ for } g, g' \in \mathcal{X}_\infty,$$

where  $L(f)$  is the Lipschitz constant of  $f$ , cf. [1, Lemma 2].

The following result establishes the existence and uniqueness of a solution for the Cauchy problem associated with equation (8).

**Proposition 1** [1, Proposition 1] *Let  $\tau$  be a fixed positive real number. Then, for each  $X_0 \in \mathcal{X}_\infty$  there exists a unique  $X \in C([0, \tau], \mathcal{X}_\infty)$  which satisfies*

$$X(x, t) = e^{-t} X_0(x) + \int_0^t e^{-(t-s)} \mathbf{H}(X(x, s)) ds \quad (9)$$

where

$$\mathbf{H}X(x, t) = \int_{\mathbb{Z}_p} A(|x - y|_p) f(X(y, t)) dy + \int_{\mathbb{Z}_p} B(|x - y|_p) U(y) dy + Z(x). \quad (10)$$

The function  $X(x, t)$  is differentiable in  $t$  for all  $x$ , and it is a solution of equation (8) with initial datum  $X_0$ .

The following result shows the stability of the  $p$ -adic continuous CNNs.

**Theorem 2** [1, Theorem 2] *All the states  $X(x, t)$  of a  $p$ -adic continuous CNN are bounded for all time  $t \geq 0$ . More precisely, if*

$$X_{\max} := \|X_0\|_\infty + \|f\|_\infty \|A\|_1 + \|U\|_\infty \|B\|_1 + \|Z\|_\infty,$$

then

$$|X(x, t)| \leq X_{\max} \text{ for all } t \geq 0 \text{ and for all } x \in \mathbb{Z}_p. \quad (11)$$

In addition

$$X_-(x) := \liminf_{t \rightarrow \infty} X(x, t) \leq X(x, t) \leq \limsup_{t \rightarrow \infty} X(x, t) =: X_+(x),$$

for  $x \in \mathbb{Z}_p$ . If  $X_-(x) = X_+(x) := X^*(x)$ , then  $X^*(x)$  is a stationary solution of the CNN  $(A, B, U, Z)$  and

$$X^*(x) \geq -\|f\|_\infty \|A\|_1 - \|U\|_\infty \|B\|_1 + Z(x). \quad (12)$$

**Remark 3** Condition (11) implies that  $X(x, t)$  does not blow-up at finite time. The existence of a stationary state  $X^*(x)$  means that the state of each cell of a  $p$ -adic continuous CNN most settle at stable equilibrium point after the transient has decayed to zero.

### 3.3 A Numerical simulation

For an in-depth discussion of the numerical methods use in the numerical simulations given in this article, the reader may consult [1]-[2].

The discretization of the kernels  $A$ , and  $B$  are functions on  $G_l \times G_l$ , while the input  $U$  and initial condition  $X_0$  are functions on  $G_l$ . We use heat maps to visualize these functions. Since  $G_l$  is isomorphic to  $\mathbb{Z}/p^l\mathbb{Z}$ , we identify the leaves of the tree with the set  $\{0, 1, \dots, p^l - 1\}$ . We also include a tree plot that represents  $G_l$ .

In this example, we take  $l = 5$ ,  $p = 3$ , which means we use a tree with  $3^5 = 243$  leaves and 5 levels. A basic application of the classical CNNs is image processing, [5]. In this example we present a one-dimensional edge detector, which is a  $p$ -adic, one-dimensional analog of the examples 3.1 and 3.2 in [5]. The input (the image) is

$$U(x) = \cos(6\pi M(x)),$$

where  $M(x) : \mathbb{Z}_p \rightarrow [0, 1]$  is the Monna map. As in [5], we take  $X_0(x) = 0$ . To construct templates  $A$  and  $B$ , we identify a matrix with a test function. We use

$$A(x) = 2\Omega(3^5|x|_p), \quad B(x) = 3^5 (3^3\Omega(3^5|x|_p) - \Omega(3^3|x|_p)).$$

Finally, we take  $Z(x) = -\Omega(3^5|x|_p)$ ,  $f(x) = 0.5(|x+1| - |x-1|)$ . The output  $Y(x, t)$  consists of the edges on the input  $U$ ; see Figures 4-6.

## 4 Reaction-diffusion CNNs with delay

In this section, we present an extension of the  $p$ -adic continuous CNNs. The new networks include a  $p$ -adic diffusion term and delay.

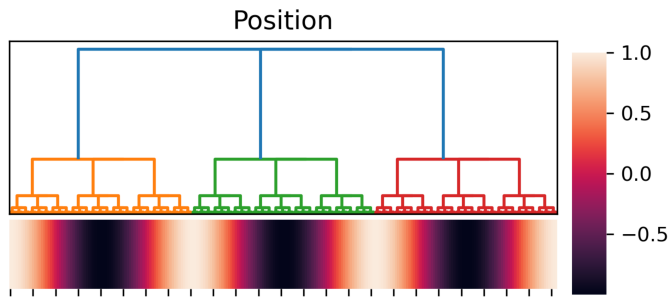


Figure 4: Heat map of  $U(x)$ . The position of each neuron corresponds with a leave of  $G_5$ . Time 25 and step  $\delta_t = 0.05$ .

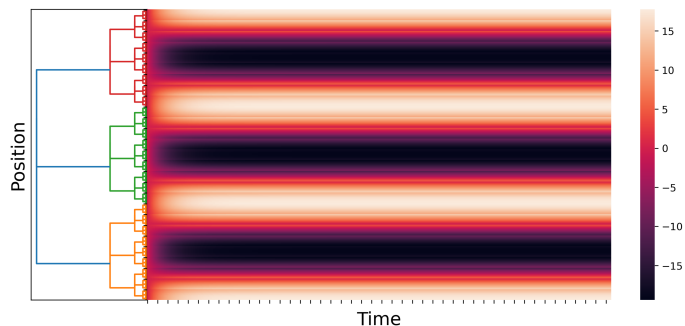


Figure 5: Heat map of  $X(x, t)$ . Time 25 and step  $\delta_t = 0.05$ .

## 5 Heat-type equations on the unit ball

We fix a function  $J : \mathbb{Z}_p \rightarrow [0, \infty)$  satisfying  $\int_{\mathbb{Z}_p} J(x) dx = 1$ . We attach to this function the operator:

$$\mathbf{J}f(x) = \int_{\mathbb{Z}_p} J(x-y) \{f(y) - f(x)\} dy.$$

We now consider the equation

$$\frac{\partial u(x, t)}{\partial t} = \mathbf{J}u(x, t). \quad (13)$$

This equation describes an ultradiffusion (or  $p$ -adic diffusion) process in  $\mathbb{Z}_p$ . Considering  $u(x, t)$  as a density of individuals or particles at the point  $x$  and interpreting  $J(x-y)$  as the probability distribution of jumping from location  $y$  to location  $x$ , the amount  $\int_{\mathbb{Z}_p} J(x-y)u(y, t)dy$  is the rate at which particles

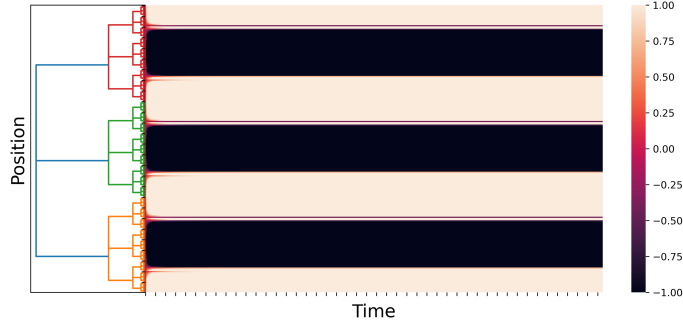


Figure 6: Heat map of  $Y(x, t)$ . Time 25 and step  $\delta_t = 0.05$ .

are arriving at position  $x$  from all other places, and  $-u(x, t) = -\int_{\mathbb{Z}_p} J(x - y)u(y, t)dy$  is the rate at which they are leaving the location  $x$  to travel to other places. Assuming that there are no creation or inhalation of particles, i.e., in the absence of external or internal sources, the density  $u(x, t)$  must satisfy the differential equation (13). Equations of type appeared in several  $p$ -adic models of complex systems, see, e.g., [30], [36]-[38], [44]-[47]. Nowadays, there is a very general theory for equations of type (13). Here, we need a particular case of Theorem 3.1 from [36]:

**Theorem 4** *Consider the Cauchy problem:*

$$\begin{cases} u(x, t) \in C^1([0, T], C(\mathbb{Z}_p, \mathbb{R})) \\ \frac{du(x, t)}{dt} = \mathbf{J}u(x, t), t \in [0, T], x \in \mathbb{Z}_p \\ u(x, 0) = u_0(x) \in C(\mathbb{Z}_p, \mathbb{R}_+) \end{cases} \quad (14)$$

where  $T \in [0, \infty]$ . There exists a probability measure  $p_t(x, \cdot)$ ,  $t \in [0, T]$ , with  $T = T(u_0)$ ,  $x \in \mathbb{Z}_p$ , on the Borel  $\sigma$ -algebra of  $\mathbb{Z}_p$ , such that the Cauchy problem (14) has a unique solution of the form

$$h(x, t) = \int_{\mathbb{Z}_p} u_0(y)p_t(x, dy).$$

In addition,  $p_t(x, \cdot)$  is the transition function of a Markov process  $\mathfrak{X}$  whose paths are right continuous and have no discontinuities other than jumps.

## 6 $p$ -Adic reaction-diffusion CNNs with delay

In this section, we use a sigmoidal function  $f : \mathbb{R} \rightarrow \mathbb{R}$ , which is a continuous function satisfying: (i)  $\lim_{t \rightarrow \pm\infty} f(t)$  exists; (ii)  $f$  is globally Lipschitz function, i.e.,  $|f(t_2) - f(t_1)| \leq L|t_2 - t_1|$ , where  $L$  is a positive constant; (iii)  $f(0) = 0$ .

Sigmoidal functions of type  $f(t) = \frac{1}{2}(|t+1| - |t-1|)$  are widely used in the framework of CNNs. Notice that  $f$  is bounded.

Given  $A(x, y), B(x, y) \in C(\mathbb{Z}_p \times \mathbb{Z}_p, \mathbb{R})$ , and  $U(x), Z(x) \in C(\mathbb{Z}_p, \mathbb{R})$ ,  $\lambda \geq 0$ , a  $p$ -adic reaction-diffusion CNN, denoted as  $CNN(J, f, \lambda, A, B, U, Z)$ , is the dynamical system given by the following system integrodifferential equations: (i) state equation:

$$\begin{aligned} \frac{\partial X(x, t)}{\partial t} = & -\lambda X(x, t) + \mathbf{J}X(x, t) + \int_{\mathbb{Z}_p} A(x, y)Y(y, t + \theta)dy \\ & + \int_{\mathbb{Z}_p} B(x, y)U(y)dy + Z(x), \end{aligned} \quad (15)$$

for  $x \in \mathbb{Z}_p, t \geq 0, \theta \in [-r, 0]$ , for some  $r > 0$ , and  $X(x, s) = \varphi(x, s), x \in \mathbb{Z}_p, -r \leq s \leq 0$ , and (ii) output equation

$$Y(x, t + \theta) = \begin{cases} f(X(x, t + \theta)), & x \in \mathbb{Z}_p, t \geq 0 \\ f(\varphi(x, s)) & x \in \mathbb{Z}_p, -r \leq s \leq 0, \end{cases} \quad (16)$$

where  $\varphi(x, s) \in C(\mathbb{Z}_p \times [-r, 0], \mathbb{R})$ . We say that  $X(x, t) \in \mathbb{R}$  is the *state of cell*  $x$  at the time  $t$ ,  $Y(x, t) \in \mathbb{R}$  is the *output of cell*  $x$  at the time  $t$ . Function  $A(x, y)$  is the *kernel of the feedback operator*, while function  $B(x, y)$  is the *kernel of the feedforward operator*. Function  $U$  is the *input of the CNN*, while function  $Z$  is the *threshold of the CNN*. The parameter  $\theta \in [-r, 0]$  gives the time delay.

In the case  $A(x, y) = A(|x - y|_p)$  and  $B(x, y) = B(|x - y|_p)$ , we say that the CNN is space invariant.

## 6.1 Discrete versions

To obtain a discretization of (15)-(16), we fix a time horizon  $\tau \in (0, \infty)$ , and take

$$X(x, t) = \sum_{i \in G_t} X(i, t) \Omega(p^l |x - i|_p), \quad X(i, t) \in C^1([-r, \tau], \mathbb{R}) \text{ for } i \in G_t, \quad (17)$$

$$Y(x, t) = f(X(x, t)) = \sum_{i \in G_t} f(X(i, t)) \Omega(p^l |x - i|_p), \quad (18)$$

$$J(x) = \sum_{i \in G_t} J(i) \Omega(p^l |x - i|_p), \quad (19)$$

$$A(x, y) = \sum_{k \in G_t} \sum_{j \in G_t} A(k, j) \Omega(p^l |x - k|_p) \Omega(p^l |y - j|_p), \quad (20)$$

$$B(x, y) = \sum_{k \in G_t} \sum_{j \in G_t} B(k, j) \Omega(p^l |x - k|_p) \Omega(p^l |y - j|_p), \quad (21)$$



$$Z(x) = \sum_{k \in G_l} Z(k) \Omega(p^l |x - k|_p), \quad U(x) = \sum_{k \in G_l} U(k) \Omega(p^l |x - k|_p). \quad (22)$$

Then, by using (ii) For very

$$\Omega(p^l |x - i|_p) * \Omega(p^l |x - j|_p) = p^{-l} \Omega(p^l |x - (i + j)|_p), \quad \text{for } i, j \in G_l,$$

and formulas (17)-(19),

$$\begin{aligned} & -\lambda X(x, t) + \mathbf{J}X(x, t) = J * X(x, t) - (\lambda + 1) X(x, t) \\ &= \sum_{i \in G_l} \sum_{j \in G_l} p^{-l} J(i) X(j, t) \Omega(p^l |x - (i + j)|_p) - (\lambda + 1) \sum_{k \in G_l} X(k, t) \Omega(p^l |x - k|_p) \\ &= \sum_{k \in G_l} \sum_{i \in G_l} p^{-l} J(i) X(k - i, t) \Omega(p^l |x - k|_p) - (\lambda + 1) \sum_{k \in G_l} X(k, t) \Omega(p^l |x - k|_p) \\ &= \sum_{k \in G_l} \left\{ \sum_{i \in G_l} p^{-l} J(i) X(k - i, t) - (\lambda + 1) X(k, t) \right\} \Omega(p^l |x - k|_p), \end{aligned}$$

and by using (18) and (20),

$$\begin{aligned} & \int_{\mathbb{Z}_p} A(x, y) Y(y, t + \theta) dy = \\ & \sum_{k \in G_l} \left\{ \sum_{j \in G_l} A(k, j) f(X(j, t + \theta)) \int_{\mathbb{Z}_p} \Omega(p^l |y - j|_p) dy \right\} \Omega(p^l |x - k|_p) \\ &= \sum_{k \in G_l} \left\{ \sum_{j \in G_l} p^{-l} A(k, j) f(X(j, t + \theta)) \right\} \Omega(p^l |x - k|_p), \end{aligned}$$

and by using (21)-(22),

$$\int_{\mathbb{Z}_p} B(x, y) U(y) dy + Z(x) = \sum_{k \in G_l} \left\{ \sum_{i \in G_l} p^{-l} B(k, i) U(i) + Z(k) \right\} \Omega(p^l |x - k|_p).$$

Finally, the discretization of (15)-(16) takes the following form:

$$\begin{cases} \frac{\partial}{\partial t} X(k, t) = -(\lambda + 1) X(k, t) + \sum_{i \in G_l} p^{-l} J(i) X(k - i, t) \\ \quad \quad \quad + \sum_{i \in G_l} p^{-l} A(k, i) Y(i, t + \theta) + \sum_{i \in G_l} p^{-l} B(k, i) U(i) + Z(k) \\ Y(k, t + \theta) = f(X(k, t + \theta)), \end{cases} \quad (23)$$

for  $k \in G_l$ .

Using matrix notation:

$$\mathbf{X}(t) = [X(k, t)]_{k \in G_l}, \quad \mathbf{Y}(t + \theta) = [Y(k, t + \theta)]_{k \in G_l}, \quad \mathbf{J} = [J(k)]_{k \in G_l},$$

$\mathbf{U} = [U(k)]_{k \in G_l}$ ,  $\mathbf{Z} = [Z(k)]_{k \in G_l}$ ,  $\mathbf{A} = [A(k, i)]_{k, i \in G_l}$ ,  $\mathbf{B} = [B(k, i)]_{k, i \in G_l}$ ,

the system (23) can be rewritten as

$$\begin{cases} \frac{\partial}{\partial t} \mathbf{X}(t) = -(\lambda + 1) \mathbf{X}(t) + p^{-l} \mathbf{J} * \mathbf{X}(t) + p^{-l} \mathbf{A} \mathbf{Y}(t + \theta) + \mathbf{B} \mathbf{U} + \mathbf{Z} \\ \mathbf{Y}(t + \theta) = [f(X(k, t + \theta))]_{k \in G_l}. \end{cases}$$

## 6.2 A class of reaction-diffusion equations with delay

Given a Banach space  $(\mathcal{X}, \|\cdot\|_{\mathcal{X}})$  and  $r > 0$ , we denote by  $C([-r, 0], \mathcal{X})$ , the Banach space of  $\mathcal{X}$ -valued functions on  $[-r, 0]$  with the supremum norm:

$$\|f\| = \sup_{s \in [-r, 0]} \|f(s)\|_{\mathcal{X}}. \quad (24)$$

In the case  $\mathcal{X} = \mathbb{R}$ , we denote norm (24) as  $\|f\|_{\infty}$ . We set  $C(\mathbb{Z}_p, \mathbb{R})$  for the Banach space of real valued functions on  $\mathbb{Z}_p$  with the supremum norm:

$$\|h\|_{\infty} = \sup_{x \in \mathbb{Z}_p} |h(x)|.$$

The results presented in this section are valid for arbitrary Banach spaces  $(\mathcal{X}, \|\cdot\|_{\mathcal{X}})$ . However, we apply the results in two cases:

$$(\mathcal{X}, \|\cdot\|_{\mathcal{X}}) = (C(\mathbb{Z}_p, \mathbb{R}), \|\cdot\|_{\infty}), \quad (\mathcal{D}^l(\mathbb{Z}_p), \|\cdot\|_{\infty}) = (\mathcal{D}^l(\mathbb{Z}_p, \mathbb{R}), \|\cdot\|_{\infty}) \simeq (\mathbb{R}^{p^l}, \|\cdot\|).$$

Notice that

$$(\mathcal{D}^l(\mathbb{Z}_p, \mathbb{R}), \|\cdot\|_{\infty}) \hookrightarrow (C(\mathbb{Z}_p, \mathbb{R}), \|\cdot\|_{\infty}),$$

where the arrow denotes a continuous embedding.

Along this section, we work with ‘delayed functions’ of type  $u(x, t + \theta)$ , where  $u$  is a continuous function,  $x \in \mathbb{Z}_p$ ,  $t \in [a, b]$ , with  $a < b$ , and  $\theta \in [-r, 0]$ . We identify this function with an element of  $C([-r, 0], C(\mathbb{Z}_p \times [a - r, b], \mathbb{R}))$  parametrized by  $x \in \mathbb{Z}_p$  given by

$$u_t(x)(\theta) = u(x, t + \theta) \text{ for } \theta \in [-r, 0], t \geq 0.$$

Then,  $u : [a - r, b] \rightarrow C(\mathbb{Z}_p, \mathbb{R})$  is a continuous function.

We denote by  $\mathbf{D}$  the infinitesimal generator of a  $C_0$ -semigroup  $\{\mathcal{T}_t\}_{t \geq 0}$  on  $C(\mathbb{Z}_p, \mathbb{R})$ .

We now identify  $C(\mathbb{Z}_p \times [-r, 0], \mathbb{R})$  with  $\mathcal{C} := C([-r, 0], C(\mathbb{Z}_p, \mathbb{R}))$  and set

$$\begin{aligned} F : C([-r, 0], C(\mathbb{Z}_p, \mathbb{R})) &\rightarrow C(\mathbb{Z}_p, \mathbb{R}) \\ \phi &\rightarrow F(x, \phi(x, \cdot)). \end{aligned}$$

We assume that  $F$  is globally Lipschitz in  $C(\mathbb{Z}_p, \mathbb{R})$ , that is,

$$\|F(\phi) - F(\psi)\|_{C(\mathbb{Z}_p, \mathbb{R})} \leq L_0 \|\phi - \psi\|_{\mathcal{C}}, \quad (25)$$

for  $\phi, \psi \in \mathcal{C}$ .

We now consider the following system of reaction-diffusion equations with delay on the  $p$ -adic unit ball:

$$\begin{cases} \frac{\partial u(x,t)}{\partial t} = \mathbf{D}u(x,t) + F(x, u_t(x)), & x \in \mathbb{Z}_p, t > 0 \\ u(x,s) = \varphi(x,s), & x \in \mathbb{Z}_p, -r \leq s \leq 0, \end{cases}$$

where  $\varphi(x,s) \in C(\mathbb{Z}_p \times [-r, 0], \mathbb{R})$ . Since the boundary of the unit ball  $\mathbb{Z}_p$  is the empty set, we do not need boundary conditions.

**Proposition 5** *Assuming (25), and that  $\mathbf{D}$  is the infinitesimal generator of a  $C_0$ -semigroup  $\{\mathcal{T}_t\}_{t \geq 0}$  on  $C(\mathbb{Z}_p, \mathbb{R})$ . Then, for  $t \in [0, \tau]$ , with  $\tau > 0$  arbitrary, and  $\varphi \in \mathcal{C}$ , there exists a unique continuous function  $u : [-r, \tau] \rightarrow C(\mathbb{Z}_p, \mathbb{R})$  which is a solution of the following initial value problem:*

$$\begin{cases} u(t) = \mathcal{T}(t)\varphi(\cdot, 0) + \int_0^t \mathcal{T}(t-s)F(u_s)ds, & 0 \leq t \leq \tau \\ u(0) = \varphi(\cdot, 0). \end{cases} \quad (26)$$

**Proof.** See [48, Theorem 1.1]. ■

The solution of (26) is called a *mild solution*.

We set

$$\mathcal{C}_l := C([-r, 0], \mathcal{D}^l(\mathbb{Z}_p, \mathbb{R})) \hookrightarrow \mathcal{C}.$$

Then

$$\mathcal{C}_l = \left\{ f \in \mathcal{C}; f(x, \theta) = \sum_{k \in G_l} f(k, \theta) \Omega(p^l |x - k|_p), f(k, \cdot) \in C([-r, 0], \mathbb{R}) \right\}.$$

**Proposition 6** *Assuming that*

$$F : \mathcal{C}_l \rightarrow \mathcal{D}^l(\mathbb{Z}_p, \mathbb{R})$$

$$\phi \rightarrow f(x, \phi(x, \cdot)).$$

*$F$  is globally Lipschitz in  $\mathcal{D}^l(\mathbb{Z}_p, \mathbb{R})$ , see (25), and that  $\mathbf{D}$  is the infinitesimal generator of a  $C_0$ -semigroup  $\{\mathcal{T}_t\}_{t \geq 0}$  on  $\mathcal{D}^l(\mathbb{Z}_p, \mathbb{R})$ . Then, for  $t \in [0, \tau]$ , with  $\tau > 0$  arbitrary, and  $\varphi(\cdot, 0) \in \mathcal{C}_l$ , there exists a unique continuous function  $u : [-r, \tau] \rightarrow \mathcal{D}^l(\mathbb{Z}_p, \mathbb{R})$  which is a solution of the initial value problem (26).*

**Proof.** See [48, Theorem 1.1]. ■

### 6.3 The Cauchy Problem

In this section we study the Cauchy problem (15)-(16).

**Lemma 7** Using the notation  $\mathcal{C} = C(\mathbb{Z}_p \times [-r, 0], \mathbb{R})$  as before. The mapping

$$F : \quad \mathcal{C} \quad \rightarrow \quad \mathcal{C}$$

$$\phi(x, \theta) \rightarrow \int_{\mathbb{Z}_p} A(x, y) f(\phi(y, \theta)) dy + \int_{\mathbb{Z}_p} B(x, y) U(y) dy + Z(x).$$

is well-defined and continuous, and satisfies

$$|F(\phi) - F(\psi)| \leq \|A\|_\infty L \|\phi - \psi\|_\infty,$$

for any  $\phi, \psi \in \mathcal{C}$ .

**Proof.** By using that  $|A(x, y) f(\phi(y, \theta))| \leq \|A\|_\infty \|f\|_\infty \Omega(|y|_p)$ ,  $|B(x, y) U(y)| \leq \|B\|_\infty \|U\|_\infty \Omega(|y|_p)$ , and the dominated convergence theorem, we conclude that  $(F(\phi))(x, \theta)$  is a continuous function. Now,

$$\begin{aligned} |F(\phi) - F(\psi)| &\leq \int_{\mathbb{Z}_p} |A(x, y)| |f(\phi(y, \theta)) - f(\psi(y, \theta))| dy \\ &\leq \|A\|_\infty L \int_{\mathbb{Z}_p} |(\phi(y, \theta)) - (\psi(y, \theta))| dy \\ &\leq \|A\|_\infty L \sup_{y \in \mathbb{Z}_p} \sup_{\theta \in [-r, 0]} |(\phi(y, \theta)) - (\psi(y, \theta))| = \|A\|_\infty L \|\phi - \psi\|_\infty. \end{aligned}$$

■

**Lemma 8** Assuming that  $A(x, y), B(x, y) \in \mathcal{D}^l(\mathbb{Z}_p \times \mathbb{Z}_p, \mathbb{R})$ ,  $U(x), Z(x) \in \mathcal{D}^l(\mathbb{Z}_p, \mathbb{R})$ , and using the notation  $\mathcal{C}_l = C([-r, 0], \mathcal{D}^l(\mathbb{Z}_p, \mathbb{R}))$  as before. The mapping

$$F : \quad \mathcal{C}_l \quad \rightarrow \quad \mathcal{D}^l(\mathbb{Z}_p \times [-r, 0], \mathbb{R})$$

$$\phi(x, \theta) \rightarrow \int_{\mathbb{Z}_p} A(x, y) f(\phi(y, \theta)) dy + \int_{\mathbb{Z}_p} B(x, y) U(y) dy + Z(x).$$

is well-defined and continuous, and satisfies

$$|F(\phi) - F(\psi)| \leq \|A\|_\infty L \|\phi - \psi\|_\infty,$$

for any  $\phi, \psi \in \mathcal{C}_l$ .

**Proof.** The proof is completely similar to the one given for Lemma 7. To show that the range of map  $F$  is contained in  $\mathcal{D}^l(\mathbb{Z}_p \times [-r, 0], \mathbb{R})$ , we use the discretization formulas given in Section 6.1. ■

**Theorem 9** *With the notation of Propositions 5-6, taking  $\mathcal{X}$  to be  $C(\mathbb{Z}_p, \mathbb{R})$  or  $\mathcal{D}^l(\mathbb{Z}_p, \mathbb{R})$ , and assuming that  $\mathbf{D}$  is the infinitesimal generator of a  $C_0$ -semigroup  $\{\mathcal{T}_t\}_{t \geq 0}$  on  $X$ . We take  $\varphi \in \mathcal{C}$ , if  $\mathcal{X} = C(\mathbb{Z}_p, \mathbb{R})$ , and  $\varphi \in \mathcal{C}_l$ , if  $\mathcal{X} = \mathcal{D}^l(\mathbb{Z}_p, \mathbb{R})$ . Then, for  $t \in [0, \tau]$ , with  $\tau > 0$  arbitrary, there exists a unique solution of the initial value problem*

$$\left\{ \begin{array}{l} u \in C([-r, \tau], \text{Dom}(\mathbf{D})) \cap C^1([-r, \tau], \mathcal{X}) \\ \frac{\partial u(t)}{\partial t} = \mathbf{D}u(x, t) + \int_{\mathbb{Z}_p} A(x, y) f(u_t(y, \theta)) dy + \\ \int_{\mathbb{Z}_p} B(x, y) U(y) dy + Z(x), x \in \mathbb{Z}_p, 0 \leq t \leq \tau \\ u(0) = \phi(x, 0). \end{array} \right. \quad (27)$$

satisfying (26).

**Proof.** The first step is to show that a solution of (27), i.e., that a classical solution, is a mild solution (26). This follows from Lemmas 7-8, by using [49, Theorem 5.1.1]. In the second step, one shows the existence of an unique mild solution, cf. Propositions 5- 6. In the third step, one shows that the mild solution (26) is differentiable. This follows from the fact that  $\int_0^t \mathcal{T}(t-s) F(u_s) ds$  is differentiable, which in turn follows from the fact that  $F(u_s)$  is integrable, see [49, Corollary 4.7.5], since

$$\begin{aligned} |F(u_s)(x)| &= \left| \int_{\mathbb{Z}_p} A(x, y) f(u_s(y)) dy + \int_{\mathbb{Z}_p} B(x, y) U(y) dy + Z(x) \right| \\ &\leq \|A\|_\infty \|f\|_\infty + \|B\|_\infty \|U\|_\infty + \|Z\|_\infty. \end{aligned}$$

Finally, the uniqueness of the solution of Cauchy problem (27) follows from the uniqueness of the mild solution, cf. Propositions 5-6. ■

**Corollary 10** *Set  $\mathcal{X}$  to be  $C(\mathbb{Z}_p, \mathbb{R})$  or  $\mathcal{D}^l(\mathbb{Z}_p, \mathbb{R})$ , and  $\mathbf{D} = \mathbf{J}$ ,  $\mathcal{T}_t = e^{t\mathbf{J}}$ ,  $t \geq 0$ , on  $\mathcal{X}$ . We take  $\varphi \in \mathcal{C}$ , if  $\mathcal{X} = C(\mathbb{Z}_p, \mathbb{R})$ , and  $\varphi \in \mathcal{C}_l$ , if  $\mathcal{X} = \mathcal{D}^l(\mathbb{Z}_p, \mathbb{R})$ . In this last case, take  $A(x, y), B(x, y) \in \mathcal{D}^l(\mathbb{Z}_p \times \mathbb{Z}_p, \mathbb{R})$ ,  $J(x)$ ,  $U(x)$ ,  $Z(x) \in \mathcal{D}^l(\mathbb{Z}_p, \mathbb{R})$ . Then, for  $t \in [0, \tau]$ , with  $\tau > 0$  arbitrary, there exists a unique*

solution of the initial value problem

$$\left\{ \begin{array}{l} X \in C^1([-r, \tau], \mathcal{X}) \\ \frac{\partial X(x, t)}{\partial t} = (\mathbf{J} - \lambda) X(x, t) + \int_{\mathbb{Z}_p} A(x, y) f(X(y, t + \theta)) dy \\ \quad + \int_{\mathbb{Z}_p} B(x, y) U(y) dy + Z(x), \quad x \in \mathbb{Z}_p, t \in [0, \tau], \theta \in [-r, 0] \\ X(x, 0) = X_0(x, 0) \in C([-r, 0], \mathcal{X}) \end{array} \right.$$

satisfying

$$X(x, t) = e^{t(\mathbf{J} - \lambda)} X_0(x, 0) + \int_0^t e^{(t-s)(\mathbf{J} - \lambda)} \left\{ \int_{\mathbb{Z}_p} A(x, y) f(X(x, s + \theta)) dy + \int_{\mathbb{Z}_p} B(x, y) U(y) dy + Z(x) \right\} ds,$$

for  $x \in \mathbb{Z}_p$ ,  $t \in [0, \tau]$ ,  $\theta \in [-r, 0]$ .

#### 6.4 Stability of CNNs with delay

**Theorem 11** *If  $\lambda > \|J\|_1 = 1$ , all the states  $X(x, t)$  of a CNN( $\lambda, J, A, B, U, Z$ ) are bounded for all time  $t \geq 0$ . More precisely, if*

$$X_{\max} := \|A\|_{\infty} \|f\|_{\infty} + \|B\|_{\infty} \|U\|_{\infty} + \|Z\|_{\infty},$$

then

$$\sup_{t \geq 0} \sup_{x \in \mathbb{Z}_p} |X(x, t)| \leq \frac{X_{\max}}{\lambda - \|J\|_1}. \quad (28)$$

If  $A(x, y), B(x, y) \in \mathcal{D}^l(\mathbb{Z}_p \times \mathbb{Z}_p, \mathbb{R})$ ,  $J(x), U(x), Z(x) \in \mathcal{D}^l(\mathbb{Z}_p, \mathbb{R})$ ,

$$X_{\max} = \|f\|_{\infty} \max_{i, k \in G_l} |A(i, k)| + \max_{i, k \in G_l} |B(i, k)| \max_{i \in G_l} |U(i)| + \max_{i \in G_l} |Z(i)|.$$

**Proof.** Set  $X_{\max} := \|A\|_{\infty} \|f\|_{\infty} + \|B\|_{\infty} \|U\|_{\infty} + \|Z\|_{\infty}$ , then, the result follows from Corollary 10 by using

$$\begin{aligned} |X(x, t)| &\leq e^{t(\|J\|_1 - \lambda)} \|X_0\|_{\infty} + X_{\max} \int_0^t e^{(t-s)(\|J\|_1 - \lambda)} \\ &= e^{-t(\lambda - \|J\|_1)} \|X_0\|_{\infty} + X_{\max} \begin{cases} t & \text{if } \lambda = \|J\|_1 \\ \frac{1 - e^{-(\lambda - \|J\|_1)t}}{\lambda - \|J\|_1} & \text{if } \lambda > \|J\|_1 \\ \frac{(e^{(\|J\|_1 - \lambda)t} - 1)}{\|J\|_1 - \lambda} & \text{if } \lambda < \|J\|_1. \end{cases} \end{aligned}$$

■

## 6.5 Some numerical examples

In this section, we present some numerical approximations for the solution of the Cauchy problem (27). We use the numerical techniques developed in ([1])-( [2]). The time step used  $\delta_t = 0.05$ , and the time runs through the ninterval  $[0, 30]$ . We use  $p = 2$ , and use truncated 2-adic numbers with five digits,  $l = 5$ ; these numbers correspond to the vertices at the top level of the tree  $G_5$ . We also use

$$J(x) = \begin{cases} 2^2 & \text{if } |x|_2 \leq 2^{-2} \\ 0 & \text{otherwise,} \end{cases}$$

$$\begin{aligned} U(x) &= \sin(\pi(1 - |x|_2)), \quad A(x) = -4 \sin(\pi(1 - |x|_2)), \\ B(x) &= \cos(\pi(1 - |x|_2)), \quad Z(x) = -0.15\Omega(|x|_2), \end{aligned}$$

$$\phi(x, s) = \begin{cases} \cos(\pi|x|_2) \cdot \sin(\pi \cdot s) & \text{if } |x|_2 \leq 2^{-3} \\ \exp(-|x|_2) \cdot \sin(\pi \cdot s) & \text{otherwise,} \end{cases}$$

where  $x \in \mathbb{Z}_p$ , and  $s \in [-4, 0]$ , thus  $r = -4$ . We use  $\lambda = 0.5, 2.0$ . The numerical experiments show that in  $p$ -adic CNNs without delay the steady state response of the network does not depend on the initial datum  $\phi(x, 0)$ ; while in case with delay, the steady state response depend heavily on the ‘memory  $\phi(x, s)$ .’ The memory induces a ‘chaotic type’ steady state response in the network.

## 7 Applications of $p$ -adic CNNs in image processing: edge detection

In this section, we review the edge detectors based on  $p$ -adic CNNs for grayscale images introduced in [2]. We take  $B \in L^1(\mathbb{Z}_p)$  and  $U, Z \in \mathcal{C}(\mathbb{Z}_p)$ ,  $a, b \in \mathbb{R}$ , and fix the sigmoidal function  $f(s) = \frac{1}{2}(|s + 1| - |s - 1|)$  for  $s \in \mathbb{R}$ . In this section, we consider the following  $p$ -adic CNN:

$$\begin{cases} \frac{\partial}{\partial t} X(x, t) = -X(x, t) + aY(x, t) + (B * U)(x) + Z(x), & x \in \mathbb{Z}_p, t \geq 0; \\ Y(x, t) = f(X(x, t)). \end{cases} \quad (29)$$

We denote this  $p$ -adic CNN as  $CNN(a, B, U, Z)$ , where  $a, B, U, Z$  are the parameters of the network. In applications to edge detection, we take  $U(x)$  to be a grayscale image, and take the initial datum as  $X(x, 0) = 0$ . The simulations show that after a time sufficiently large the network outputs a white and black image approximating the edges of the original image  $U(x)$ . The performance of this edge detector is comparable to the Canny detector, and other well-know detectors. But most importantly, they can explain, reasonably well, how the network learns the edges of an image.

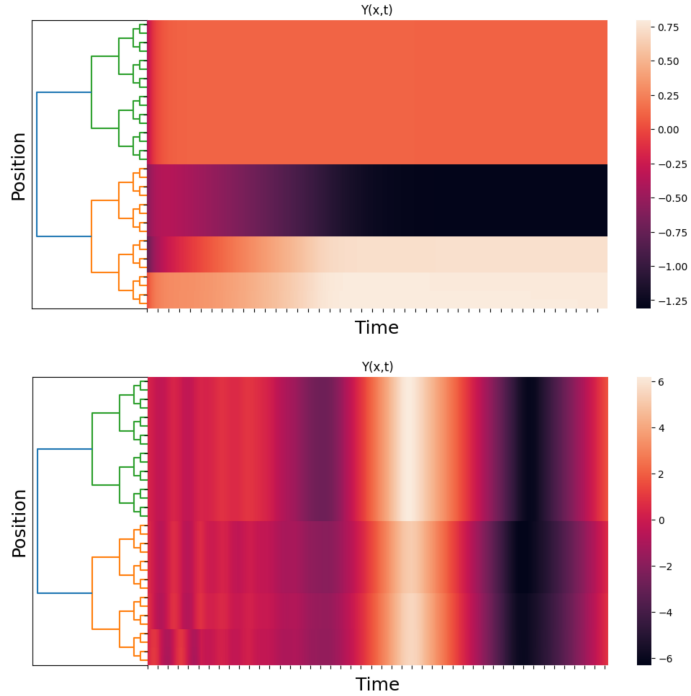


Figure 7: The top figure is the response of the network with no delay, i.e.  $r = 0$ . The bottom figure is the response of the network with  $r = -4$ . In both cases  $\lambda = 0.5$ .

## 7.1 Stationary states

We say that  $X_{stat}(x)$  is a *stationary state* of the network  $CNN(a, B, U, Z)$ , if

$$\begin{cases} X_{stat}(x) = aY_{stat}(x) + (B * U)(x) + Z(x), & x \in \mathbb{Z}_p; \\ Y_{stat}(x) = f(X_{stat}(x)). \end{cases} \quad (30)$$

**Lemma 12** [2, Lemma 1](i) *If  $a < 1$ , then the network  $CNN(a, B, U, Z)$  has a unique stationary state  $X_{stat}(x) \in \mathcal{C}(\mathbb{Z}_p)$  given by*

$$X_{stat}(x) = \begin{cases} a + (B * U)(x) + Z(x) & \text{if } (B * U)(x) + Z(x) > 1 - a \\ -a + (B * U)(x) + Z(x) & \text{if } (B * U)(x) + Z(x) < -1 + a \\ \frac{(B * U)(x) + Z(x)}{1 - a} & \text{if } |(B * U)(x) + Z(x)| \leq 1 - a. \end{cases} \quad (31)$$

(ii) *If  $a = 1$ , then the network  $CNN(a, B, U, Z)$  has a unique stationary state*



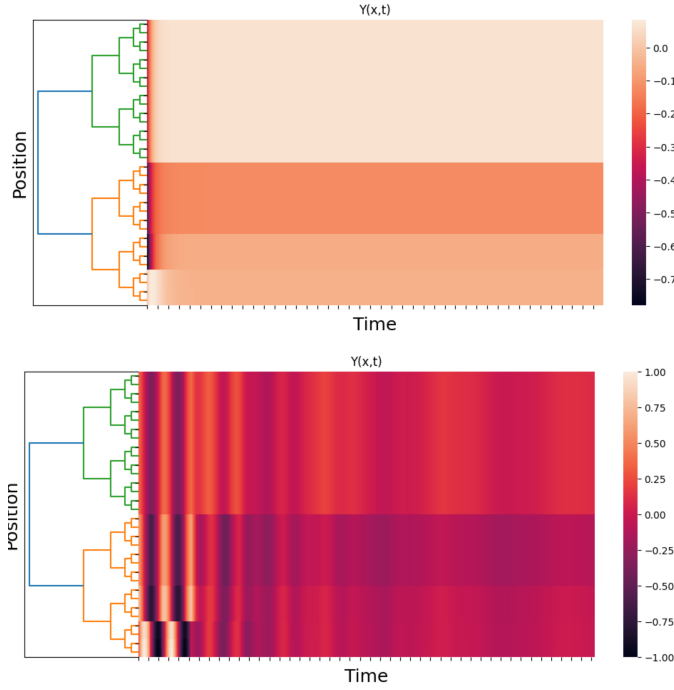


Figure 8: The top figure is the response of the network with no delay, i.e.  $r = 0$ . The bottom figure is the response of the networks with  $r = -4$ . In both cases  $\lambda = 2.0$ .

$X_{stat}(x) \in L^1(\mathbb{Z}_p)$  given by

$$X_{stat}(x) = \begin{cases} 1 + (B * U)(x) + Z(x) & \text{if } (B * U)(x) + Z(x) > 0 \\ -1 + (B * U)(x) + Z(x) & \text{if } (B * U)(x) + Z(x) < 0 \\ 0 & \text{if } (B * U)(x) + Z(x) = 0. \end{cases} \quad (32)$$

**Definition 13** Assume that  $a > 1$ . Given

$$I_+ \subseteq \{x \in \mathbb{Z}_p; 1 - a < (B * U)(x) + Z(x)\},$$

$$I_- \subseteq \{x \in \mathbb{Z}_p; (B * U)(x) + Z(x) < a - 1\},$$

satisfying  $I_+ \cap I_- = \emptyset$  and

$$\mathbb{Z}_p \setminus (I_+ \cup I_-) \subseteq \{x \in \mathbb{Z}_p; 1 - a < (B * U)(x) + Z(x) < a - 1\},$$

we define the function

$$X_{stat}(x; I_+, I_-) = \begin{cases} a + (B * U)(x) + Z(x) & \text{if } x \in I_+ \\ -a + (B * U)(x) + Z(x) & \text{if } x \in I_- \\ \frac{(B * U)(x) + Z(x)}{1 - a} & \text{if } x \in \mathbb{Z}_p \setminus (I_+ \cup I_-). \end{cases} \quad (33)$$

**Theorem 14** [2, Theorem 1] Assume that  $a > 1$ . All functions of type (33) are stationary states of the network  $CNN(a, B, U, Z)$ . Conversely, any stationary state of the network  $CNN(a, B, U, Z)$  has the form (33).

**Remark 15** Notice that

$$Y_{stat}(x; I_+, I_-) := f(X_{stat}(x; I_+, I_-)) = \begin{cases} 1 & \text{if } x \in I_+ \\ -1 & \text{if } x \in I_- \\ \frac{(B*U)(x)+Z(x)}{1-a} & \text{if } x \in \mathbb{Z}_p \setminus (I_+ \cup I_-). \end{cases}$$

The function  $Y_{stat}(x; I_+, I_-)$  is the output of the network. If  $I_+ \cup I_- = \mathbb{Z}_p$ , we say that  $X_{stat}(x; I_+, I_-)$  is bistable. The set  $\mathcal{B}(I_+, I_-) = \mathbb{Z}_p \setminus (I_+ \cup I_-)$  measures how far  $X_{stat}(x; I_+, I_-)$  is from being bistable. We call set  $\mathcal{B}(I_+, I_-)$  the set of bistability of  $X_{stat}(x; I_+, I_-)$ . If  $\mathcal{B}(I_+, I_-) = \emptyset$ , then  $X_{stat}(x; I_+, I_-)$  is bistable.

**Remark 16** If  $I_+ \cup I_- \subsetneq \mathbb{Z}_p$ , we say that  $X_{stat}(x; I_+, I_-)$  is an unstable.

## 7.2 Hierarchical structure of the space of stationary states

A relation  $\preceq$  is a *partial order* on a set  $S$  if it satisfies: 1 (reflexivity)  $f \preceq f$  for all  $f$  in  $S$ ; 2 (antisymmetry)  $f \preceq g$  and  $g \preceq f$  implies  $f = g$ ; 3 (transitivity)  $f \preceq g$  and  $g \preceq h$  implies  $f \preceq h$ . A *partially ordered set*  $(S, \preceq)$  (or poset) is a set endowed with a partial order. A partially ordered set  $(S, \preceq)$  is called a *lattice* if for every  $f, g$  in  $S$ , the elements  $f \wedge g = \inf\{f, g\}$  and  $f \vee g = \sup\{f, g\}$  exist. Here,  $f \wedge g$  denotes the smallest element in  $S$  satisfying  $f \wedge g \preceq f$  and  $f \wedge g \preceq g$ ; while  $f \vee g$  denotes the largest element in  $S$  satisfying  $f \preceq f \vee g$  and  $g \preceq f \vee g$ . We say that  $h \in S$  a *minimal* element of with respect to  $\preceq$ , if there is no element  $f \in S$ ,  $f \neq h$  such that  $f \preceq h$ .

Posets offer a natural way to formalize the notion of hierarchy.

We set

$$\mathcal{M} = \bigcup_{I_+, I_-} \{X_{stat}(x; I_+, I_-)\},$$

where  $I_+, I_-$  run through all the sets given in Definition 13. Given  $X_{stat}(x; I_+, I_-)$  and  $X_{stat}(x; I'_+, I'_-)$  in  $\mathcal{M}$ , with  $I_+ \cup I_- \neq \mathbb{Z}_p$  or  $I'_+ \cup I'_- \neq \mathbb{Z}_p$ , we define

$$X_{stat}(x; I'_+, I'_-) \preceq X_{stat}(x; I_+, I_-) \text{ if } I_+ \cup I_- \subseteq I'_+ \cup I'_-. \quad (34)$$

In the case  $I_+ \cup I_- = \mathbb{Z}_p$  and  $I'_+ \cup I'_- = \mathbb{Z}_p$ , the corresponding stationary states  $X_{stat}(x; I_+, I_-)$ ,  $X_{stat}(x; I'_+, I'_-)$  are not comparable. In [2], the authors show that (34) defines a partial order in  $\mathcal{M}$ .

**Theorem 17** [2, Theorem 2]  $(\mathcal{M}, \preceq)$  is a lattice. Furthermore, the set of minimal elements of  $(\mathcal{M}, \preceq)$  agrees with the set of bistable states of  $CNN(a, B, U, Z)$ .

### 7.3 A new class of edge detectors

In [2, Theorem 2], the authors implemented a numerical method for solving the initial value problem attached to network  $CNN(a, B, U, Z)$ , with  $X(x, 0) = 0$  and  $U(x)$  a grayscale image. The simulations show that after a sufficiently large time the network outputs a black-and-white image approximating the edges of the original image  $U(x)$ . This means that for  $t$  sufficiently large  $X(x, t)$  is close to a bistable stationary state  $X_{stat}(x; I_+, I_-)$ . Furthermore, after a certain sufficiently large time, the output of the network do not show a difference perceivable by the human eye. See Figures 9-10. The performance of this edge detector is comparable to the Canny detector, and other well-known detectors. But most importantly, we can explain, reasonably well, how the network detects the edges of an image.

An intuitive picture of the dynamics of the network is as follows. For  $t$  sufficiently large, the network performs transitions between stationary states  $X_{stat}(x; I_+, I_-)$  belonging to a small neighborhood  $\mathcal{N}$  around a bistable state  $X_{stat}^{(0)}(x; I_+, I_-)$ , with  $I_+ \cup I_- = \mathbb{Z}_p$ . The dynamics of the network consists of transitions in a hierarchically organized landscape  $(\mathcal{M}, \preceq)$  toward some minimal state. This is a reformulation of the classical paradigm asserting that the dynamics of a large class of complex systems can be modeled as a random walk on its energy landscape.



Figure 9: Left side, the original image. Right side, edges obtained by using a Canny edge detector. Taken from [2].

## 8 Applications of $p$ -adic CNNs in image processing: edge detection: denoising

In this section, we review the filtering techniques introduced in [2] for grayscale images polluted with Gaussian noise.

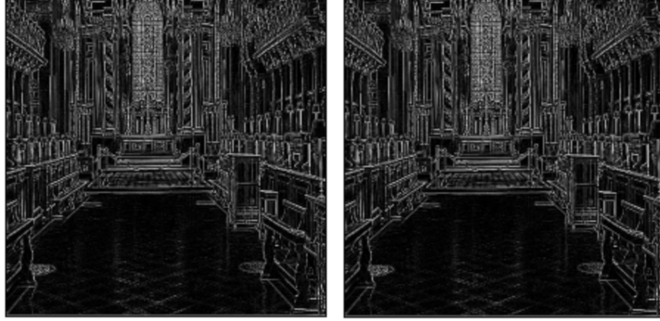


Figure 10: On the left side, edges were obtained by using a discretization of the CNN (29), with  $z_0 = -1$  and 6 steps. On the right side, edges were obtained by using a discretization of the CNN (29), with  $z_0 = -1$  and 10 steps. See [2] for further details.

### 8.1 The $p$ -adic heat equation

The field of  $p$ -adic numbers  $\mathbb{Q}_p$  is the quotient field of the ring  $\mathbb{Z}_p$ :

$$\mathbb{Q}_p = \left\{ \frac{a}{b}; a, b \in \mathbb{Z}_p, \text{ with } b \neq 0 \right\}.$$

Any  $p$ -adic number  $x \neq 0$  has a unique expansion of the form

$$x = p^{\text{ord}_p(x)} \sum_{j=0}^{\infty} x_j p^j, \quad (35)$$

where  $x_j \in \{0, 1, 2, \dots, p-1\}$ ,  $x_0 \neq 0$ , and  $\text{ord}_p(x) = \text{ord}(x) \in \mathbb{Z}$ . It follows from (35), that any  $x \in \mathbb{Q}_p \setminus \{0\}$  can be represented uniquely as  $x = p^{\text{ord}(x)} u(x)$  and  $|x|_p = p^{-\text{ord}(x)}$ .

We denote by  $\mathcal{D}(\mathbb{Q}_p)$  the  $\mathbb{R}$ -vector space of test functions defined on  $\mathbb{Q}_p$ ,  $L^2(\mathbb{Q}_p)$  the  $\mathbb{R}$ -vector space of square integrable functions defined on  $\mathbb{Q}_p$ , and by  $C(\mathbb{Q}_p)$  the  $\mathbb{R}$ -vector space of continuous functions defined on  $\mathbb{Q}_p$ .

For  $\alpha > 0$ , the Vladimirov-Taibleson operator  $\mathbf{D}^\alpha$  is defined as

$$\begin{aligned} \mathcal{D}(\mathbb{Q}_p) &\rightarrow L^2(\mathbb{Q}_p) \cap C(\mathbb{Q}_p) \\ \varphi &\rightarrow \mathbf{D}^\alpha \varphi, \end{aligned}$$

where

$$(\mathbf{D}^\alpha \varphi)(x) = \frac{1 - p^\alpha}{1 - p^{-\alpha-1}} \int_{\mathbb{Q}_p} \frac{[\varphi(x-y) - \varphi(x)]}{|y|_p^{\alpha+1}} dy.$$

The  $p$ -adic analogue of the heat equation is

$$\frac{\partial u(x, t)}{\partial t} + a \mathbf{D}^\alpha u(x, t) = 0, \text{ with } a > 0.$$

The solution of the Cauchy problem attached to the heat equation with initial datum  $u(x, 0) = \varphi(x) \in \mathcal{D}(\mathbb{Q}_p)$  is given by

$$u(x, t) = \int_{\mathbb{Q}_p} Z(x - y, t) \varphi(y) dy,$$

where  $Z(x, t)$  is the  $p$ -adic heat kernel defined as

$$Z(x, t) = \int_{\mathbb{Q}_p} \chi_p(-x\xi) e^{-at|\xi|_p^\alpha} d\xi, \quad (36)$$

where  $\chi_p(-x\xi)$  is the standard additive character of the group  $(\mathbb{Q}_p, +)$ . The  $p$ -adic heat kernel is the transition density function of a Markov stochastic process with space state  $\mathbb{Q}_p$ , see, e.g., [50]-[51].

## 8.2 The $p$ -adic heat equation on the unit ball

We define the operator  $\mathbf{D}_0^\alpha$ ,  $\alpha > 0$ , by restricting  $\mathbf{D}^\alpha$  to  $\mathcal{D}(\mathbb{Z}_p)$  and considering  $(\mathbf{D}^\alpha \varphi)(x)$  only for  $x \in \mathbb{Z}_p$ . The operator  $\mathbf{D}_0^\alpha$  satisfies

$$\mathbf{D}_0^\alpha \varphi(x) = \lambda \varphi(x) + \frac{1 - p^\alpha}{1 - p^{-\alpha-1}} \int_{\mathbb{Z}_p} \frac{\varphi(x - y) - \varphi(x)}{|y|_p^{\alpha+1}} dy,$$

for  $\varphi \in \mathcal{D}(\mathbb{Z}_p)$ , with  $\lambda = \frac{p-1}{p^{\alpha+1}-1} p^\alpha$ .

Consider the Cauchy problem

$$\begin{cases} \frac{\partial u(x, t)}{\partial t} + \mathbf{D}_0^\alpha u(x, t) - \lambda u(x, t) = 0, & x \in \mathbb{Z}_p, \quad t > 0; \\ u(x, 0) = \varphi(x), & x \in \mathbb{Z}_p, \end{cases}$$

where  $\varphi \in \mathcal{D}(\mathbb{Z}_p)$ . The solution of this problem is given by

$$u(x, t) = \int_{\mathbb{Z}_p} Z_0(x - y, t) \varphi(y) dy, \quad x \in \mathbb{Z}_p, \quad t > 0,$$

where

$$\begin{aligned} Z_0(x, t) &:= e^{\lambda t} Z(x, t) + c(t), \quad x \in \mathbb{Z}_p, \\ c(t) &:= 1 - (1 - p^{-1}) e^{\lambda t} \sum_{n=0}^{\infty} \frac{(-1)^n}{n!} t^n \frac{1}{1 - p^{-n\alpha-1}} \end{aligned}$$

and  $Z(x, t)$  is given (36). The function  $Z_0(x, t)$  is non-negative for  $x \in \mathbb{Z}_p, t > 0$ , and

$$\int_{\mathbb{Z}_p} Z_0(x, t) dx = 1,$$

[50]. Furthermore,  $Z_0(x, t)$  is the transition density function of a Markov process with space state  $\mathbb{Z}_p$ .

The family

$$\begin{aligned} T_t : L^1(\mathbb{Z}_p) &\rightarrow L^1(\mathbb{Z}_p) \\ \phi(x) &\rightarrow T_t \phi(x) := \int_{\mathbb{Z}_p} Z_0(x - y, t) \phi(y) dy, \end{aligned} \quad (37)$$

is a  $C^0$ -semigroup of contractions with generator  $\mathbf{D}_0^\alpha - \lambda I$  on  $L^1(\mathbb{Z}_p)$ , see [52, Proposition 4, Proposition 5]

### 8.3 Reaction-diffusion CNNs

Given  $\mu \in \mathbb{R}, \alpha > 0, A, B, U, Z \in \mathcal{C}(\mathbb{Z}_p)$ , a  $p$ -adic reaction-diffusion CNN, denoted as  $CNN(\mu, \alpha, A, B, U, Z)$ , is the dynamical system given by the following integro-differential equation:

$$\begin{aligned} \frac{\partial X(x, t)}{\partial t} &= \mu X(x, t) + (\lambda I - \mathbf{D}_0^\alpha) X(x, t) + \int_{\mathbb{Z}_p} A(x - y) f(X(y, t)) dy \\ &+ \int_{\mathbb{Z}_p} B(x - y) U(y) dy + Z(x), \end{aligned} \quad (38)$$

where  $x \in \mathbb{Z}_p, t \geq 0$ . We say that  $X(x, t) \in \mathbb{R}$  is the state of cell  $x$  at the time  $t$ . Function  $A$  is the kernel of the feedback operator, while function  $B$  is the kernel of the feedforward operator. Function  $U$  is the input of the CNN, while function  $Z$  is the threshold of the CNN.

Notice that if  $\mu = 0$  and  $A = B = U = Z = 0$ , (38) becomes the  $p$ -adic heat equation in the unit ball. Then, in (38),  $(\lambda I - \mathbf{D}_0^\alpha)$  is the diffusion term, while the other terms are the reaction ones, which describe the interaction between  $X(x, t), U(x)$ , and  $Z(x)$ .

The following result establishes the existence of uniqueness of a mild solution for the Cauchy problem associated with (38). This result is sufficient to study the stability of these networks.

**Proposition 18** [2, Proposition 1, Lemma 3](i) *Let  $A, B, U, Z \in \mathcal{C}(\mathbb{Z}_p)$ . Take  $X_0 \in L^1(\mathbb{Z}_p)$  as the initial datum for the Cauchy problem attached to (38). Then there exists  $\tau = \tau(X_0) \in (0, \infty]$  and a unique  $X(t) \in C([0, \tau], L^1(\mathbb{Z}_p))$  satisfying*

$$\begin{cases} X(t) = e^{\mu t} T_t X_0 + \int_0^t e^{\mu(t-s)} T_{t-s} \mathbf{H}(X(s)) ds \\ X(0) = X_0. \end{cases} \quad (39)$$

(ii) Let  $A, B, U, Z \in C(\mathbb{Z}_p)$ . Take  $X_0 \in C(\mathbb{Z}_p)$ . Then, the integral equation (39) has unique solution  $C([0, \infty), C(\mathbb{Z}_p))$ .

**Theorem 19** [2, Theorem 3] Let  $X(t) \in C([0, \infty), C(\mathbb{Z}_p))$  be the unique solution of (39), with initial condition  $X_0 \in C(\mathbb{Z}_p)$ . Then,

$$\|X(t)\|_\infty \leq e^{\mu t} \|X_0\|_\infty + \frac{(e^{\mu t} - 1)}{\mu} (\|A\|_1 \|f\|_\infty + \|B\|_1 \|U\|_\infty + \|Z\|_\infty), \quad (40)$$

if  $\mu \neq 0$ , otherwise

$$\|X(t)\|_\infty \leq \|X_0\|_\infty + \tau (\|A\|_1 \|f\|_\infty + \|B\|_1 \|U\|_\infty + \|Z\|_\infty). \quad (41)$$

## 8.4 Denoising

In this section, we review the denoising technique based on reaction-diffusion CNNs introduced in [2]. We first consider the initial value problem

$$\begin{cases} \frac{\partial X(x,t)}{\partial t} + D_0^1 X(x,t) - \lambda X(x,t) = 0, & x \in \mathbb{Z}_p, \quad t > 0 \\ X(x,0) = X_0(x), & x \in \mathbb{Z}_p, \end{cases} \quad (42)$$

where  $X_0(x) \in [0, 1]$  is a grayscale image codified as a test function supported in the unit ball  $\mathbb{Z}_p$ . The algorithm for this coding is discussed in [2]. The output image  $X(x, t)$  is similar to the one produced by the classical Gaussian filter. See Figure 11.



Figure 11: On the left side, the original image  $X(x, 0)$ . On the right side  $X(x, 3)$ . Taken from [2].

In [2] was proposed the following reaction-diffusion CNN for denoising grayscale images polluted with normal additive noise:

$$\frac{\partial X(x,t)}{\partial t} = 3X(x,t) + (\lambda I - D_0^3)X(x,t) + 3B * [X_0(x) - f(X(x,t))], \quad (43)$$

where  $\alpha = 0.75$ ,  $f(x) = 0.5(|x+1| - |x-1|)$ ,  $B(x) = (\Omega(p^2|x|_p) - \Omega(|x|_p))$ , and  $-1 \leq X_0(x) \leq 1$ . Notice that we are using the interval  $[-1, 1]$  as a grayscale scale. This equation was found experimentally. Natively, the reaction term  $3X(x, t) + 3B * [X_0(x) - f(X(x, t))]$  gives an estimation of the edges of the image, while the diffusion term  $(\lambda I - D_0^\alpha)X(x, t)$  produces a smoothed version of the image.

The processing of an image  $X_0(x)$  using (43) requires solving the corresponding Cauchy problem with initial datum  $X(x, 0) = X_0(x)$ . For an in-depth discussion on the numerical and computational techniques required, the reader may consult [2]. See Figure 12.



Figure 12: Left side, the original image. Right side, the image plus Gaussian noise, mean zero and variance 0.05. Taken from [2].

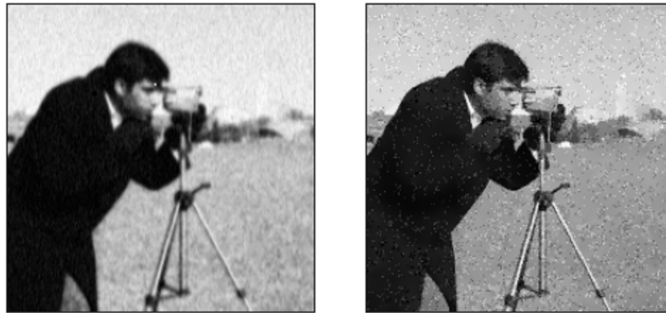


Figure 13: Left side, filtered image using Equation 43. Right side, filtered image obtained by using Perona-Malik equation with  $\lambda = 0.04$ ,  $\delta_t = 0.075$ , and  $t = 100$  iterations, and  $g_1(s)$ , see [53]. Taken from [2].



## 9 $p$ -Adic Wilson-Cowan Models and Connection Matrices

In [19], the Wilson-Cowan models were formulated on Abelian, locally compact topological groups, see model 4. The classical model corresponds to the group  $(\mathbb{R}, +)$ . Using classical techniques on semilinear evolution equations, see e.g. [48]-[49], it was showed that the corresponding Cauchy problem is locally well-posed, and if  $r_E = r_I = 0$ , it is globally well-posed, see [19, Theorem 1]. This last condition corresponds to the case of two coupled perceptrons.

We already discussed in Section 2.2 that the compatibility of the Wilson-Cowan model with the small-world network property requires a non-negligible interaction between any two groups of neurons, in turn, this fact requires that the neurons be organized in compact group. Now,  $(\mathbb{R}^N, +)$  does not have non-trivial compact subgroups. Indeed, if  $x_0 \neq 0$ , then  $\langle x_0 \rangle = \{nx_0; n \in \mathbb{Z}\}$  is a non-compact subgroup of  $(\mathbb{R}^N, +)$ , because  $\{|n|; n \in \mathbb{Z}\}$  is not bounded. This last assertion is equivalent to the Archimedean axiom of the real numbers. In conclusion, the compatibility between the Wilson-Cowan model and the small-world property requires changing  $(\mathbb{R}, +)$  to a compact Abelian group. In [19], the authors selected the field of the  $p$ -adic numbers. This field has infinitely many compact subgroups, the balls with center at the origin. They selected the unit ball, the ring of  $p$ -adic numbers  $\mathbb{Z}_p$ .

The  $p$ -adic Wilson-Cowan model admits good discretizations. Each discretization corresponds to a system of non-linear integrodifferential equations on a finite rooted tree. They show that the solution of the Cauchy problem of this discrete system provides a good approximation to the solution of the Cauchy problem of the  $p$ -adic Wilson-Cowan model, see [19, Theorem 2]. They provide extensive numerical simulations of  $p$ -adic Wilson-Cowan models that show that the  $p$ -adic models provide a similar explanation to the numerical experiments presented in [21]. They also show that the connection matrices can be incorporated into the  $p$ -adic Wilson-Cowan model.

## 10 Some open problems

### 10.1 Traveling waves for neural networks

The existence and uniqueness of traveling waves for model 1 have been the focus of great interest; see, e.g., [54]-[57], and the references therein. A such solution has the form  $u(x, t) = v(x - ct)$ , where  $c$  is the speed of the wave. In the  $p$ -adic framework, studying such solutions is an open problem. Time-independent traveling waves (called bumps) are localized solutions. This type of solution has also been studied intensively; see, e.g., [58]-[62], and the references therein. The study of this type of solution is also an open problem in the  $p$ -adic framework.

## 10.2 Fuzzy CNNs

In [63]-[64], the fuzzy cellular neural networks (FCNNs) were introduced as an extension of the CNNs. The FCNNs use fuzzy operators in the synaptic law that combine the low-level information processing capability of the CNNs with the high-level information processing capability, such as image understanding, of fuzzy systems. The FCNNs has been used in many different applications, for instance, in edge detection for noised images [64]-[65], segmentation of medical images [66]-[67], and image encryption, see [68]-[69], among several applications.

We propose the following formulation for the  $p$ -adic version of the FCNNs:

$$\begin{aligned} \frac{\partial X(x,t)}{\partial t} = & -aX(x,t) + A(x) * f(X(x,t)) + B(x) * U(x) + Z(x) \\ & + \bigvee_z \left( A_{max}(z) * f(X(z,t)) \Omega(p^{l(x)}|z-x|_p) \right) \\ & + \bigvee_z \left( B_{max}(z) * U(z) \Omega(p^{l(x)}|z-x|_p) \right) \\ & + \bigwedge_z \left( A_{min}(z) * f(X(z,t)) \Omega(p^{l(x)}|z-x|_p) \right) \\ & + \bigwedge_z \left( B_{min}(z) * U(z) \Omega(p^{l(x)}|z-x|_p) \right), \end{aligned}$$

where  $X(x,t)$  and  $f(X(x,t))$  are the state and output of cell  $x \in \mathbb{Z}_p$  at time  $t$ , respectively;  $f: \mathbb{R} \rightarrow \mathbb{R}$  is a bounded Lipschitz function satisfying  $f(0) = 0$ ;  $U(x)$  and  $Z(x)$  are the input and threshold of cell  $x \in \mathbb{Z}_p$ ;  $A, B \in \mathcal{C}(\mathbb{Z}_p)$  are the feedback and feedforward kernels. Finally,  $A_{max}$ ,  $B_{max}$ ,  $A_{min}$ , and  $B_{min}$  are kernels for the local fuzzy operators  $\bigvee_z$  and  $\bigwedge_z$ . We introduce a continuous function  $l: \mathbb{Z}_p \rightarrow \mathbb{N}$  that defines the locality of the fuzzy operators. The Fuzzy operators are defined as

$$\begin{aligned} \bigvee_z \phi(z) \Omega(p^{l(x)}|z-x|_p) & := \max\{\phi(z); z \in x + p^{l(x)}\mathbb{Z}_p\}, \\ \bigwedge_z \phi(z) \Omega(p^{l(x)}|z-x|_p) & := \min\{\phi(z); z \in x + p^{l(x)}\mathbb{Z}_p\}. \end{aligned}$$

There are several open problems related with  $p$ -adic FCNNs, we just mention two. First, to study the stability and the stationary states of the of  $p$ -adic FCNNs. Second, to develop image processing algorithms based on  $p$ -adic FCNNs.

## 10.3 Chaos in CNNs with delay

The numerical experiments presented in Section 4 show that the responses of the  $p$ -adic CNNs with delay have a chaotic behavior. A relevant problem is investigating the different dynamical behaviors, including limit cycles, chaos, etc., for different ranges of parameters of the network.

## 10.4 Development of visual computing techniques based on $p$ -adic CNNs

In [1]-[2], the first two authors showed that  $p$ -adic CNNs can be used to implement edge detection and denoising algorithms. But, it is necessary to investigate the use of  $p$ -adic CNNs in general visual computing tasks, see, e.g., [5], [70].

## References

- [1] Zambrano-Luna B. A., Zúñiga-Galindo W. A.,  $p$ -adic cellular neural networks, *J. Nonlinear Math. Phys.* 30 (2023), no. 1, 34–70.
- [2] Zambrano-Luna B. A., Zúñiga-Galindo W. A.,  $p$ -adic cellular neural networks: applications to image processing, *Phys. D* 446 (2023), Paper No. 133668, 11 pp.
- [3] Chua Leon O., Yang Lin, Cellular neural networks: theory, *IEEE Trans. Circuits and Systems* 35, no. 10, 1257–1272, 1988.
- [4] Chua Leon, Yang Lin, Cellular Neural Networks: Applications, *IEEE Trans. on Circuits and Systems*, 35, no. 10, 1273-1290, 1988.
- [5] Chua Leon O, Roska, Tamas, Cellular neural networks and visual computing: foundations and applications. Cambridge university press, 2002.
- [6] Slavova Angela, Cellular neural networks: dynamics and modelling. *Mathematical Modelling: Theory and Applications*, 16. Kluwer Academic Publishers, Dordrecht, 2003.
- [7] Coobes Stephen, baim Graben Peter, Potthast Roland, and Wright James, Editors. (2014). *Neural fields. Theory and applications*. Springer, Heidelberg.
- [8] Sporns O., Tononi G., Edelman G. M. (2000). Theoretical neuroanatomy: relating anatomical and functional connectivity in graphs and cortical connection matrices, *Cerebral Cortex*, 10( 2), 127–14.
- [9] Sporns O. (2006). Small-world connectivity, motif composition, and complexity of fractal neuronal connections, *Biosystems*, 85(1), 55-64.
- [10] Sporns O, Honey C. J. (2006). Small worlds inside big brains, *Proc Natl Acad Sci USA*. 103(51):19219-20.
- [11] Hilgetag C. C., Goulas A. (2016). Is the brain really a small-world network? *Brain Struct Funct.* 221(4), 2361-6.
- [12] Muldoon S. F., Bridgeford E. W., Bassett D. S. (2016). Small-World Propensity and Weighted Brain Networks, *Sci Rep.* 6, 22057.

- [13] Bassett D. S., Bullmore E. T. (2017). Small-World Brain Networks Revisited, *Neuroscientist*, 23(5), 499-516.
- [14] Akiki T. J., Abdallah C. G. (2019). Determining the Hierarchical Architecture of the Human Brain Using Subject-Level Clustering of Functional Networks, *Sci Rep* 9, 19290.
- [15] Scannell J. W., Blakemore C., Young M. P. (1995). Analysis of connectivity in the cat cerebral cortex, *J. Neurosci.* 15(2), 1463-83.
- [16] Fornito Alex, Zalesky Andrew, Bullmore Edward T. Editors. (2016). *Connectivity Matrices and Brain Graphs in Fundamentals of Brain Network Analysis*. Academic Press. Pages 89-113.
- [17] Sporns Olaf. (2016). *Networks of the Brain*. Penguin Random House LLC, 2016.
- [18] Škoch A., Reháková B., Mareš J., Tintěra J., Sanda P., Jajcay L., Horáček J., Španiel F., Hlinka J. (2022). Human brain structural connectivity matrices-ready for modeling, *Sci Data*, 9, 486.
- [19] Zúñiga-Galindo W. A., Zambrano-Luna B. A., Hierarchical Wilson-Cowan models and connection matrices, *Entropy* 25 (2023), no. 6, Paper No. 949, 20 pp.
- [20] Wilson H. R., Cowan J. D. , Excitatory and inhibitory interactions in localized populations of model neurons, *Biophys. J.*, 12 (1972), pp. 1-23.
- [21] Wilson H. R., Cowan J. D., A mathematical theory of the functional dynamics of cortical and thalamic nervous tissue, *Kybernetik*, 13 (1973), pp. 55-80.
- [22] Amari S., Dynamics of pattern formation in lateral inhibition type neural fields, *Biol. Cybern.*, 27 (1977), pp. 77-87.
- [23] Laing, C., Troy, W., Gutkin, B., Ermentrout, G.: Multiple bumps in a neuronal model of working memory. *SIAM J. Appl. Math.* 63, 62 (2002).
- [24] Zhang K., Representation of spatial orientation by the intrinsic dynamics of the head-direction cell ensemble: a theory, *J. Neurosci.* 16(6), 2112–2126 (1996)
- [25] Ermentrout B., Neural networks as spatio-temporal pattern-forming systems, *Rep. Prog. Phys.* 61, 353 (1998).
- [26] Ermentrout G.B., Cowan J.D., A mathematical theory of visual hallucination patterns, *Biol. Cybern.* 34, 137–150 (1979).
- [27] Bojak I., Liley D.T.J., Modeling the effects of anesthesia on the electroencephalogram, *Phys. Rev. E* 71, 041,902 (2005).

- [28] Bressloff Paul C., Stochastic neural field theory and the system-size expansion, *SIAM J. Appl. Math.* 70(2009/10), no.5, 1488–1521.
- [29] Iordache O., Non-Archimedean Analysis. In: *Modeling Multi-Level Systems. Understanding Complex Systems*, vol 70. Springer, Berlin, Heidelberg, 2011. [https://doi.org/10.1007/978-3-642-17946-4\\_13](https://doi.org/10.1007/978-3-642-17946-4_13)
- [30] Khrennikov Andrei, Kozyrev Sergei, Zúñiga-Galindo W. A., *Ultrametric Equations and its Applications. Encyclopedia of Mathematics and its Applications (168)*. Cambridge University Press, 2018.
- [31] Khrennikov A., *Information Dynamics in Cognitive, Psychological, Social and Anomalous Phenomena*; Springer: Berlin/Heidelberg, Germany, 2004.
- [32] Khrennikov Andrei, Tirozzi Brunello, *Learning of  $p$ -adic neural networks. Stochastic processes, physics and geometry: new interplays, II (Leipzig, 1999)*, 395–401, *CMS Conf. Proc.*, 29, Amer. Math. Soc., Providence, RI, 2000.
- [33] Zúñiga-Galindo W. A., He C., Zambrano-Luna B. A.,  *$p$ -adic statistical field theory and convolutional deep Boltzmann machines*, *PTEP. Prog. Theor. Exp. Phys.*(2023), no. 6, Paper No. 063A01, 17 pp.
- [34] Zúñiga-Galindo W. A.,  *$p$ -adic statistical field theory and deep belief networks*, *Phys. A* 612 (2023), Paper No. 128492, 23 pp.
- [35] Zúñiga-Galindo W. A., *A Correspondence Between Deep Boltzmann Machines and  $p$ -Adic Statistical Field Theories*. To appear in *Adv. Theor. Math. Phys.* arXiv:2306.03751.
- [36] Zúñiga-Galindo, W. A., *Ultrametric diffusion, rugged energy landscapes and transition networks*, *Phys. A* 597 (2022), Paper No. 127221, 19 pp.
- [37] Zúñiga-Galindo, W. A., *Reaction-diffusion equations on complex networks and Turing patterns, via  $p$ -adic analysis*, *J. Math. Anal. Appl.* 491 (2020), no. 1, 124239, 39 pp.
- [38] Zúñiga-Galindo, W. A. *Non-Archimedean reaction-ultradiffusion equations and complex hierarchic systems*, *Nonlinearity* 31 (2018), no. 6, 2590–2616.
- [39] Alberverio S., Khrennikov A. Yu., Shelkovich V. M., *Theory of  $p$ -adic distributions: linear and nonlinear models*. London Mathematical Society Lecture Note Series, 370. Cambridge University Press, Cambridge, 2010.
- [40] Vladimirov V. S., Volovich I. V., Zelenov E. I.,  *$p$ -adic analysis and mathematical physics*. World Scientific, 1994.
- [41] Taibleson M. H., *Fourier analysis on local fields*. Princeton University Press, 1975.

- [42] Chistyakov D. V. Fractal geometry of images of continuous embeddings of  $p$ -adic numbers and solenoids into Euclidean spaces, *Theoret. and Math. Phys.* 109 (1996), no. 3, 1495–1507 (1997).
- [43] Halmos P. *Measure Theory* (D. Van Nostrand Company Inc., New York, 1950).
- [44] Torresblanca-Badillo Anselmo, Zúñiga-Galindo W. A., Ultrametric diffusion, exponential landscapes, and the first passage time problem, *Acta Appl. Math.* 157 (2018), 93–116.
- [45] Avetisov V. A., Bikulov A. Kh., Osipov V. A.,  $p$ -adic description of characteristic relaxation in complex systems, *J. Phys. A* 36, no. 15, 4239–4246, 2003.
- [46] Avetisov V. A., Bikulov A. H., Kozyrev S. V., Osipov V. A.,  $p$ -adic models of ultrametric diffusion constrained by hierarchical energy landscapes, *J. Phys. A* 35, no. 2, 177–189, 2002.
- [47] Alexander Bendikov, Heat kernels for isotropic-like Markov generators on ultrametric spaces: a survey,  *$p$ -Adic Numbers Ultrametric Anal. Appl.* 10 (2018), no. 1, 1–11.
- [48] Wu Jianhong, *Theory and applications of partial functional-differential equations*, *Appl. Math. Sci.*, 119 Springer-Verlag, New York, 1996.
- [49] Miklavčič Milan, *Applied functional analysis and partial differential equations*. World Scientific Publishing Co., Inc., River Edge, NJ, 1998.
- [50] Kochubei Anatoly N., *Pseudo-differential equations and stochastics over non-Archimedean fields*. Marcel Dekker, Inc., New York, 2001.
- [51] Zúñiga-Galindo W. A., *Pseudodifferential equations over non-Archimedean spaces*. *Lectures Notes in Mathematics* 2174, Springer, 2016.
- [52] Khrennikov Andrei Yu, Kochubei Anatoly N.,  $p$ -Adic Analogue of the Porous Medium Equation, *J Fourier Anal Appl* 24 (2018), 1401–1424.
- [53] Bredies Kristian, Lorenz Dirk, *Mathematical image processing, Applied and Numerical Harmonic Analysis*, Birkhäuser/Springer, Cham, 2018.
- [54] Ermentrout B., McLeod B., Existence and uniqueness of travelling waves for a neural network, *Proc. Roy. Soc. Edinburgh Sect. A* 123 (1993), no. 3, 461–478.
- [55] Chen Fengxin, Travelling waves for a neural network, *Electron. J. Differential Equations*(2003), No. 13, 4 pp.
- [56] Bressloff Paul C., *Waves in neural media. From single neurons to neural fields*. *Lect. Notes Math. Model. Life Sci.* Springer, New York, 2014.

- [57] Ermentrout G. Bard, Folias Stefanos E., Kilpatrick Zachary P., Spatiotemporal pattern formation in neural fields with linear adaptation. *Neural fields*, 119–151. Springer, Heidelberg, 2014.
- [58] Kishimoto K., Amari S., Existence and stability of local excitations in homogeneous neural fields. *J. Math. Biol.* 7, 303–318 (1979).
- [59] Amari, S., Dynamics of pattern formation in lateral-inhibition type neural fields, *Biol. Cybernetics* 27, 77–87 (1977).
- [60] Amari Shun-ichi, Heaviside world: excitation and self-organization of neural fields. *Neural fields*, 97–118. Springer, Heidelberg, 2014.
- [61] Laing Carlo R., PDE methods for two-dimensional neural fields. *Neural fields*, 153–173. Springer, Heidelberg, 2014.
- [62] Oleynik Anna, Ponosov, Arcady, Wyller John, Iterative schemes for bump solutions in a neural field model, *Differ. Equ. Dyn. Syst.* 23 (2015), no.1, 79–98.
- [63] Yang Tao, Yang Lin-Bao, Wu Chai Wah and Chua L. O., Fuzzy cellular neural networks: theory, 1996 Fourth IEEE International Workshop on Cellular Neural Networks and their Applications Proceedings (CNNA-96), Seville, Spain, 1996, pp. 181-186, doi: 10.1109/CNNA.1996.566545.
- [64] Yang Tao, Yang Lin-Bao, Wu Chai Wah and Chua L. O., Fuzzy cellular neural networks: applications, 1996 Fourth IEEE International Workshop on Cellular Neural Networks and their Applications Proceedings (CNNA-96), Seville, Spain, 1996, pp. 225-230, doi: 10.1109/CNNA.1996.566560.
- [65] Doan M. . -D., Halgamuge S., Glesner M. and Braunsforth S., Application of fuzzy, GA and hybrid methods to CNN template learning, 1996 Fourth IEEE International Workshop on Cellular Neural Networks and their Applications Proceedings (CNNA-96), Seville, Spain, 1996, pp. 327-332, doi: 10.1109/CNNA.1996.566594.
- [66] Shitong Wang and Min Wang, A new detection algorithm (NDA) based on fuzzy cellular neural networks for white blood cell detection, in *IEEE Transactions on Information Technology in Biomedicine*, vol. 10, no. 1, pp. 5-10, Jan. 2006, doi: 10.1109/TITB.2005.855545.
- [67] Shitong Wang, Duan Fu, Min Xu, Dewen Hu, Advanced fuzzy cellular neural network: Application to CT liver images, *Artificial Intelligence in Medicine*, vol. 39, no. 1, pp. 65–77, 2007.
- [68] Ratnavelu K., Kalpana M., Balasubramaniam P., Wong K. , and Raveendran P., Image encryption method based on chaotic fuzzy cellular neural networks, *Signal Processing*, vol. 140, pp. 87–96, 2017.

- [69] Mani P., Rajan R., Shanmugam L., and Joo Y. H., Adaptive control for fractional order induced chaotic fuzzy cellular neural networks and its application to image encryption, *Information Sciences*, vol. 491, pp. 74-89, 2019.
- [70] Itoh Makoto, Chua Leon O., Advanced Image Processing Cellular Neural Networks, *International Journal of Bifurcation and Chaos* 2007 17:04, 1109-1150.